Chapter 6

Confocal Laser Scanning Microscopy as a Tool for the Investigation of Skin Drug Delivery Systems and Diagnosis of Skin Disorders

Fábia Cristina Rossetti, Lívia Vieira Depieri and
Maria Vitória Lopes Badra Bentley

Additional information is available at the end of the chapter

http://dx.doi.org/10.5772/55995

1. Introduction

Confocal laser scanning microscopy (CLSM) is a useful image tool to study the fate of delivery systems and biomolecules applied into the skin. Through the use of fluorescence probes, it is possible to evaluate their behavior, like: i) interaction with the biological system [1]; ii) cellular uptake [2-3]; iii) depth of penetration [4]; iv) penetration routes into the skin [5]; v) quantification of skin penetration of drugs and biomolecules [6]; and vi) effect of topical therapies for several skin diseases by morphological analysis of the tissue [7].

In fluorescence microscopic terms, the skin tissue is difficult to investigate because it reflects and scatters incoming light, and melanin and other chromophores, significantly attenuate visible wavelengths [8]. CLSM has the potential to overcome these limitations, since it generates high-resolution imaging, non-invasive optical sectioning and three-dimensional reconstructions, in combination with sensitivity, selectivity and versatility of fluorescence measurements [1]. In this way, the expertise of the CLSM technique provides excellent opportunities for probing and better understanding the behavior and fate of pharmaceuticals in the skin, including *in vivo* monitoring of skin drug penetration, allowing a rational development of skin delivery systems.

This chapter intends to discuss important topics for pharmaceutical researchers related to the proper use of this technique to design and optimize skin delivery systems, as well as to diagnose skin diseases. The first topic will shortly comment about the skin structure for an easier understanding of the next ones. With the advent of nanotechnology, CLSM technique can be an imaging tool for better understanding of the fate of nanocarriers in delivering drugs

into the skin layers and the efficacy of them in the therapies of different skin disorders. Furthermore, our previous experience in this technique [9-10] will allow a critical discussion on the main topics in this specific subject and to update the advances in this field application.

2. The skin structure

The human skin is the largest organ in the body that has many important physiological functions, such as, protection (physical, chemical, immune, pathogen, UV radiation and free radical defenses), major participant in thermoregulation, sensory organ and performs endocrine functions (vitamin D synthesis, peripheral conversion of prohormones) [11]. Its thickness varies from 0.05 mm to 2 mm and is composed of four main layers: the stratum corneum (SC) and the viable epidermis, the outermost layers; the dermis, and the subcutaneous tissue (Figure 1)[12].

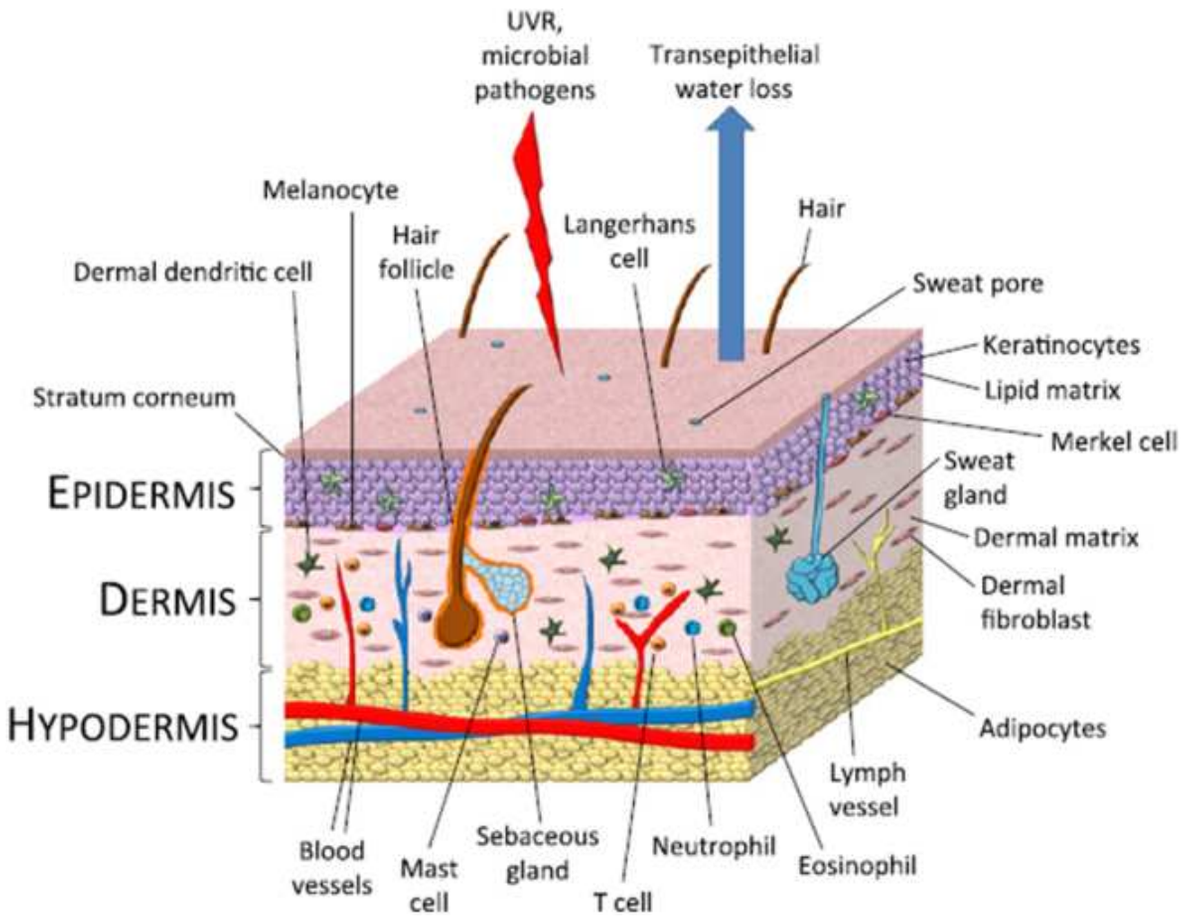

Figure 1. Schematic representation of skin structure and cell population. The skin comprises three main layers – the epidermis, dermis and hypodermis. The resident cell populations and various structures present throughout the skin allow for maintenance of an efficient barrier against water loss, and protection against threats such as ultraviolet radiation (UVR) and microbial pathogens. The blood and lymph vessels allow for the migration of immune cells in and out of the skin, so that the cell population of the skin is constantly in a state of flux, in response to the demands of the cutaneous inflammatory and immune systems. Reproduced from [13] with permission.

The SC is 10-20 μm thick, highly hydrophobic and contains 10-15 layers of interdigitated dead cells called corneocytes. It is the major barrier to penetration of drugs because its structure is highly organized [14]. Its "brick and mortar" structure is analogous to a wall. The corneocytes of hydrated keratin comprise the "bricks", embedded in a "mortar", composed of multiple lipid bilayers of ceramides, fatty acids, cholesterol and cholesterol esters. These bilayers form regions of semicrystalline, gel and liquid crystals domains. Most molecules penetrate through skin via this intercellular microroute and therefore many enhancing techniques aim to disrupt or bypass its highly organized structure [15].

The viable epidermis (~100-150 μm thick) is composed by multiple layers of keratinocytes at various stages of differentiation. Besides the keratinocytes, the epidermis also contain several other cells (melanocytes, Langerhans cells, dendritic T cells, epidermotropic lymphocytes and Merkel cells) and active catabolic enzymes (e.g. esterases, phosphatases, proteases, nucleotidases and lipases) [12].

The dermis is rich in blood vessels, nerves, hair follicles, and sebaceous and sweat glands. The elasticity of the dermis is due to the presence of collagen, elastin, glycosaminoglycans, collectively termed the extracellular matrix (ECM), as well as fibroblasts that elaborate the ECM. Dermal adipose cells, mast cells, and infiltrating leucocytes are also present in this skin layer [11-12].

3. Operational parameters for digital image capture for CLSM to assess the drug penetration into skin layers

3.1. Equipment characteristics

This technique is fluorescence-based image and offers greater resolution than fluorescence microscopy due to its point illumination and detection properties [16]. The illumination in a confocal microscopy is achieved by a collimated laser beam across the specimen [16-17]. This laser beam is reflected by a dichroic mirror and passes through the objective lens of the microscope in a focused manner on the specimen, which, and then, excites fluorescence probe in the sample. So, light is emitted at a longer wavelength which can come through the dichroic mirror and is again focused at the upper pinhole aperture (Figure 2) [16,18]. With CLSM, out-of-focus light (coming from places of the specimen above or below the focus) is cut off before the beam hits the electronic detector due to the addition of a spatial filter containing an aperture, – the pinhole or slit – the point detection. Just the light in-focus can pass through the pinhole (now termed confocal apertures), come to detector, and then form the image with more details because the blurring from out-of-focus has vanished. By using CLSM, it is possible to obtain high-resolution images (lateral, ~140 nm; axial, ~1 μm) from the samples, which increase to accuracy of the microscopic images [5,16-17].

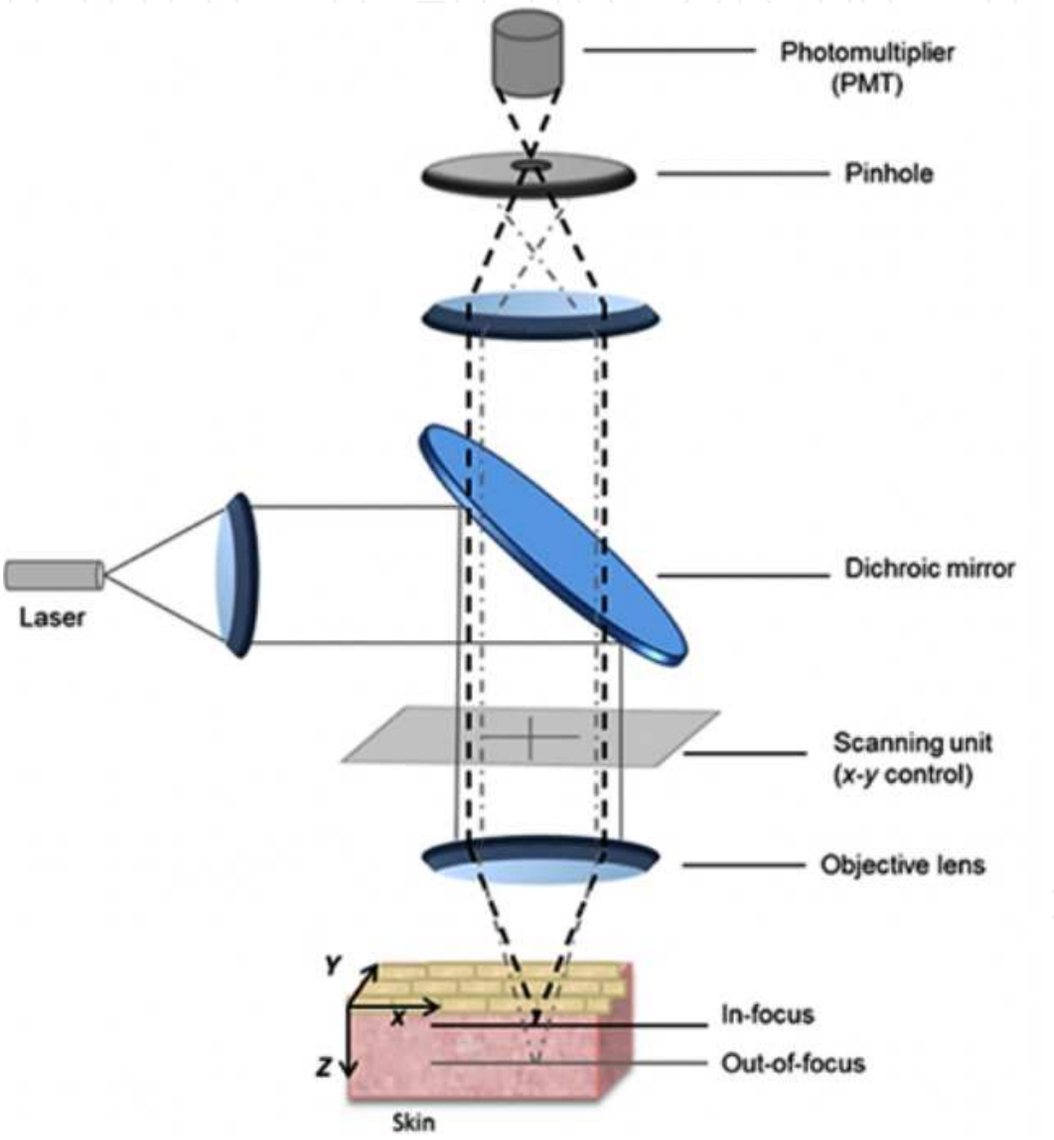

Figure 2. Schematic diagram of the principle of confocal laser scanning microscopy.

http://dx.doi.org/10.5772/55995

3.1.1. Measurement of different optical sections

Acquisition of several optical sections (*x-y* plane) taken at successive focal planes along the *z* axis is a usual practice to obtain a three-dimensional information from the skin that can be viewed as a simple image. Figure 3 shows the principle of *z* series acquisition.

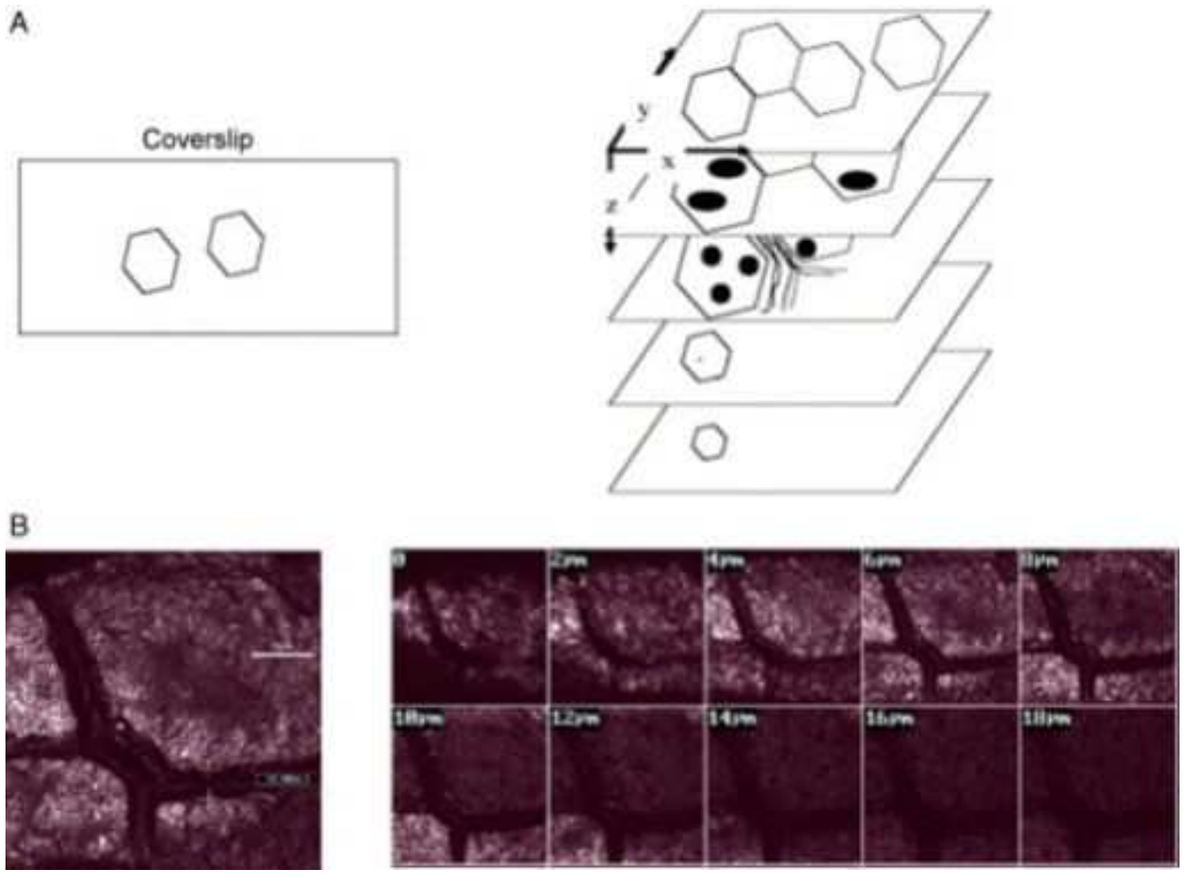

Figure 3. Confocal optical sectioning: (A) a schematic of a sample (hexagonal features) mounted on a microscope slide and covered with coverslip for a *z* series processing (sequential *x-y* sections as a function of depth (*z*); (B) confocal images of a *z* series through the porcine skin. Reproduced from [5] with permission.

Acquisition of *x-z* section is useful to obtain depth information from a specific surface. First, it is necessary to get an image in the *x-y* plane. Then, after choosing a region of interest, a horizontal line is drawn across this area in the $z = 0$ μm – *x-y* plane and is "optically sliced" through the digitalized image data of successive *x-y* sections; the results are (*x-z* planar) optical cross-sections (Figure 4).

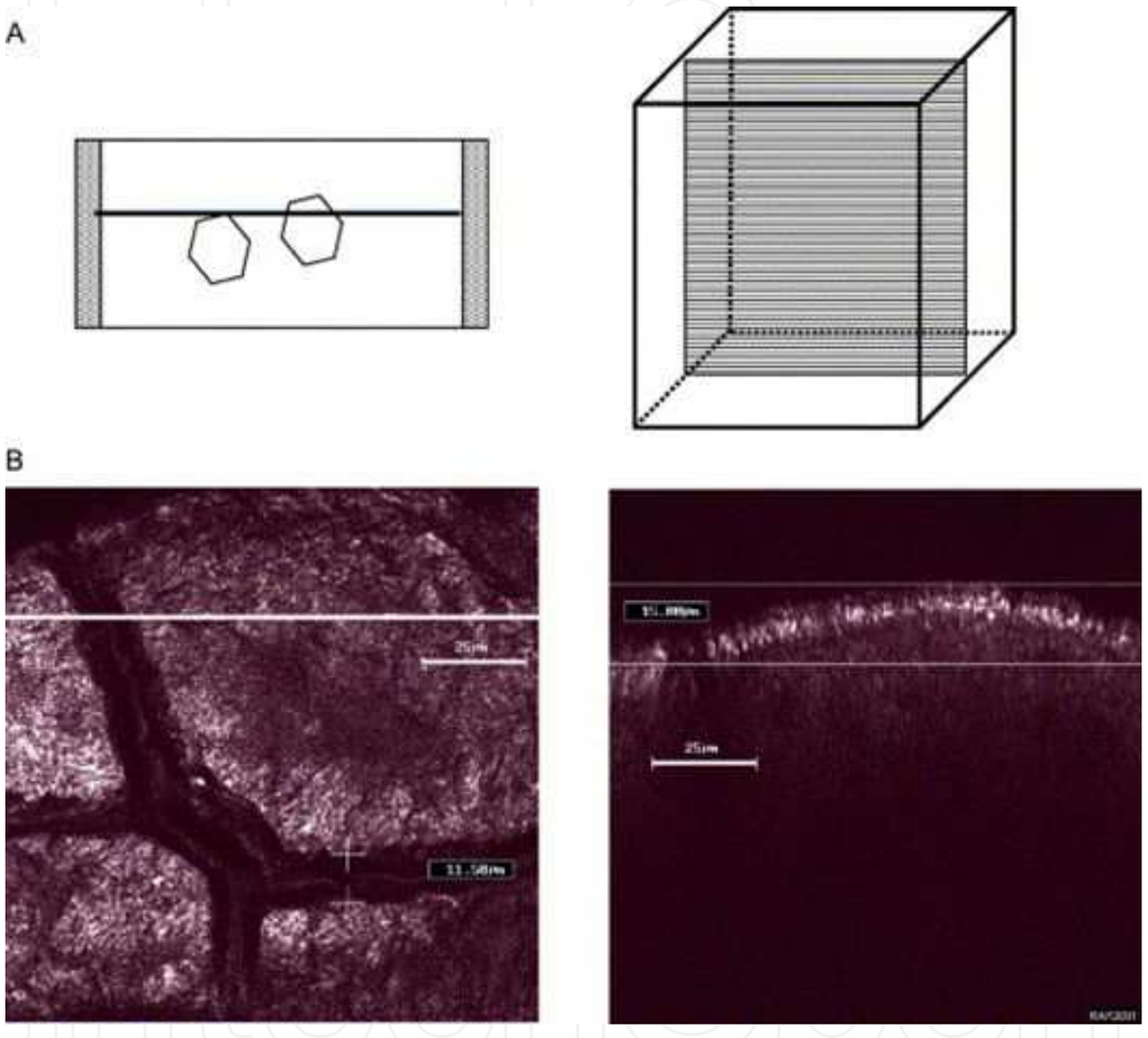

Figure 4. Confocal optical sectioning: (A) schematic of an *x-z* planar optical cross-section; (B) confocal *x-z* image of porcine skin. Reproduced from [5] with permission.

3.2. Sample processing techniques

The main goal of confocal microscopy is to explore the structure and structural relationship along the optical (*z*) axis as well in the *x-y* plane. For this, preservation of the tissues and cells during the preparation of the sample is necessary to obtain a reliable image. Optimum sample preparation is very dependent upon the cell or tissue type, the labeling technique and type of data to be collected [5,19].

Analyses by confocal microscopy can be done with living or preserved (fixed) samples. Working with living samples, is possible to analyze dynamic events and avoid some of the artifacts that can be introduced with preservation techniques and processing of the sample. It is easier to work with preserved samples since it does not have to concern about keeping the cells or tissue alive but; however, the impossibility to observe dynamic events and the presence of artifacts make this routine less attractive [19].

For skin samples, little or no sample preparation is necessary to visualize skin structures and the localization of fluorescent probes used within the tissue. Hence, the technique is rapid, with minimal physical perturbation or damage to the tissue. CLSM offers nearly accurate images with few artifacts contributing significantly in topical/transdermal permeation studies to elucidate and understand the mechanisms and pathways of drug penetration using different delivery technologies [5,19].

3.3. Main fluorescence probes used to assess skin penetration

Fluorescence is an important optical readout mode in biological confocal microscopy due to its sensitivity and specificity. These features can be influenced by the capability to tag onto biological systems to show your localization and by the local environment [20].

In some situations in which the drug carried by the delivery system studied has fluorescence properties, the use of a specific fluorophore is not necessary, once the drug can be excited and it emits fluorescence signals that are captured and transformed into image [9-10, 21].

Several fluorophores are used in skin visualization. The Table 1 shows the main used.

Objective of study	Fluorescence probe	$\lambda_{exc}/\lambda_{em}$ (nm)	Reference
Visualization and suggested mechanism of interaction between liposome-skin	β-carotene and 5(6)carboxyfluorescein	514/660-1250; 488/515-535	[22]
Evaluation of composition and preparation methods of vesicles in skin penetration	β-carotene and 5(6)carboxyfluorescein	514/660-1250; 488/515-535	[23]
Penetration and distribution of lipophilic probes in the hair follicle	Bodipy FL C_5, Bodipy 564/570 C_5 and Oregon Green	488 /514; 564/574; 488/514	[24]
Visualization of influence the use low-frequency ultrasound in skin penetration	Calcein	495/515	[25]
Evaluation the composition of liposomes in skin penetration behavior	Calcein , NBC-PC[1] and Rhodamine B	488/510; 488/530; 568/590	[26]
Visualization of penetration and distribution of nanoparticles in the skin treated with microneedles	Coumarin-6	488/	[27]
Visualization the ability of cell penetrating peptides to improve skin penetration	DID-oil	644/665	[28]
Evaluation the effect of polymeric nanoparticles with surface modified with oleic acid in skin permeation	DiO	484/501	[29]
Evaluation of skin penetration of nano lipid carries with surface modified by polyarginine	DiO	484/501	[30]

Objective of study	Fluorescence probe	$\lambda_{exc}/\lambda_{em}$ (nm)	Reference
Investigate the effect of pore number and depth on rate and extension of drug delivery through the skin using a novel laser microporation technology	FITC[2]	488/520	[31]
Influence and elucidation of the transport pathway of solute-water skin penetration with use low-frequency sonophoresis	FITC-dextran and Rhodamine B	488/520; 568/590	[32]
Evaluation of microneedle shape by visualization of skin penetration of fluorescent dye	Fluorescein	488/515	[33]
Visualization of skin penetration pathways of a novel micelle formulation	Fluorescein	505/530	[34]
Evaluation the ability of dendrimers to facilitate transdermal drug delivery *in vivo*	Fluorescein-PAMAM	488/<560	[35]
Visualization of nanoparticles deposition in a skin	Fluospheres®	405/420-480; 488/505-530; 633/647-754	[36]
Evaluation the influence of a liposome surface charge in skin penetration	NBD-PC and Rhodamine B	488/530; 568/590	[37]
Visualization the effect of heat on skin permeability	Nile red	543/630	[38]
Visualization the behavior of microemulsion formulation in the skin stratum corneum	Nile red	543/630	[39]
Visualization the behavior of polymeric particles for drug delivery to the inflamed skin	Nile red	543/595	[40]
Visualization of skin transport properties of model as a carrier for oligodeoxynucleotide (ODN) during iontophoresis	Oregon Green and TAMRA	488/505; 543/560	[6]
Evaluation the interaction of quantum dots nanoparticles in the skin	Quantum dots	351, 364, 488/610-632	[41]
Visualization the skin penetration behavior of ethosomes	Quantum dots (CdTe)	488/<560	[42]
Investigate skin penetration of quantum dots in human skin	Quantum dots (CdTe)	800/	[43]
Evaluation of ultrasound and sodium lauryl sulfate for increase transdermal delivery of nanoparticles	Cationic, neutral, and anionic quantum dots (CdSe/ZnS)		[44]
Visualization of ethosome penetration in skin and mechanism of action study	Rhodamine 6 GO	543/<560	[45]
Exploration of the three-dimensional structure, organization and barrier function of the stratum corneum *ex vivo* and *in vivo* after transfersome permeation	Rhodamine-DHPE[3], Texas Red-DHPE[4] and fluorescein-DHPE[5]	543/590; 583/601; 496/519	[46]

[1] NBD-PC=1-palmitoyl-2-{12-[(7-nitro-2-1,3-benzoxadiazol-4-yl)amino]dodecanoyl}-snglycero-3-phosphocholine.
[2] FITC=fluorescein isothiocyanate.
[3] Rhodamine-DHPE=1,2-dihexa-adecanoyl-sn-glycero-3-phosphoethanolamine-N-Lis-samine.
[4] Texas Red-DHPE=1,2-dihexa-adecanoyl-sn-glycero-3-phosphoethanolamine-N-Lis-samine.
[5] FI-DHPE=N-(5-fluoresceinthiocarbamoyl)-1,2-dihexadecanoyl-sn-glycero-3-phospho-ethanolamine.

Table 1. Main fluorescence probes used to assess skin penetration

Unfortunately, there is not a comprehensive list of available fluorophores that is selective for a particular parameter of the cell and that also has a suitable wavelength. The choice of an ideal fluorophore is not a simple task; however, it is possible to realize the choice of the more

http://dx.doi.org/10.5772/55995

appropriate fluorophore within a range of wavelengths. This selection is based on the objectives of the study taking into account the physicochemical properties of the fluorophore as well as the characteristics of the sample.

In the case of skin, various endogenous substances (Table 2) can interfere with analyzes because they are excited at a wavelength in the excitation band of the chosen fluorophores.

Fluorochrome	**$\lambda_{excitation}$ (nm)**	**$\lambda_{emission}$ (nm)**
Tryptophan	295	345
Tyrosine	275	300
Phenylalanine	260	280
Melanin	330-380	400-700
Keratin	375	430
Collagen	335	390-405
Elastin	360	460
FAD	390	520
NADH	290, 364	440, 475
NADPH	336	464
Flavoprotein	450-490	500-560
Porphyrins	476	625

Table 2. Endogenos substances responsible for the skin's autofluorescence [5]

To minimize autofluorescence of the skin, configuration settings of fluorescence detection must be made so that it can separate the fluorescence signal of the skin from that of the used fluorophore, avoiding any interference of the specimen [43]. The imaging using dual-channel and subsequent overlapping of images obtained at each channel is a resource used for reducing potential problems with autofluorescence from the sample [5]. Another resource is the choice of fluorophores with distinct emission spectra from those presented by endogenous fluorophores of the skin [47].

Some fluorophores can be covalently bound to biomolecular targets as well as the components of formulations without changing their spectral properties. The wide variety of derivatives of rhodamine and fluorescein, both well-known dyes, has been used with this subject, which result in greater functionality of these dyes [20].

Rhodamine is a lipophilic dye and because of its physicochemical property it is widely used to evaluate the dynamic properties of living cells such as membrane potential and ion concentration. It is also used to study the behavior and mechanisms of permeation of lipid delivery systems like liposomes. It can be incorporated into the lipid bilayers promoting a marking and also mimicking lipophilic drugs such as betamethasone, since they both exhibit a similar partition coefficient (log P). In many cases, it is associated with a hydrophilic dye as, for example, calcein, which is expected to be encapsulated in the aqueous compartment of the liposome, promoting marking and functioning as a model for hydrophilic drugs that can be carried by this type of delivery system [26,37].

On the other hand, fluorescein has a wide use due to its ability to react with many substrates. One example of this, it is its conjugation with dendrimers, which enables the study of the behavior and properties of dendrimer on skin permeation [35].

Moreover, for a successful CLMS analysis of the skin samples, the fluorophores probe must present: (i) good quantum efficiency and persistence of the signal sufficient for the instrument to achieve image data; (ii) selectivity for the target molecule; (iii) high resistance to bleaching; (iv) minimal perturbation to the sample; (v) minimizing the cross-talk when multiple fluorophores are being used together. Another important consideration is that the fluorescence intensity of depth images depends on both the sample transparence or opacity and the interference of the fluorescence of upper layers with the fluorescence signal of the adjacent layers [1]. Instrumentally, fluorescence emission collects can be improved by careful selection of objectives, detector aperture dimensions, dichromatic and barrier filters, as well as keeping the optical train in precise alignment [48].

3.4. Non–invasive assessment

Noninvasive optical techniques, such as CLSM, have become widely used in recent years because they are an efficient tool for skin characterization, as additional technique or even as a replacement for invasive biopsies of skin [49].

In this technique, images are obtained by scanning the specimen with one or more focus of beams of light. The images produced by this way are called optical section. This term refers to the method of collecting images noninvasively, which uses light to section the sample out instead of performing mechanical sections [17]. Due to this important characteristic, CLSM has been used in dermatology diagnosis by assessing the skin *in vivo*, where a comparison is made between the healthy skin aspect with the pathological state of living human skin [50-53].

Two modes are established for the use of *in vivo* CLSM: reflectance and fluorescence modes. The reflectance mode is based on detection of own endogenous contrast by refractive indices of several cellular structures, like melanin or keratin, which have both a high refractive index. Generally, a laser with near-infrared wavelengths is used for this type of measurements.

http://dx.doi.org/10.5772/55995

Backscattered in-focus signals are captured and transformed for the image visualization [50-51]. The fluorescence mode is based on detection of the distribution of an exogenous dye administrated before the measures. A laser beam with visible-light wavelengths is used to excite selectively the dye to produce contrast. Backscattered fluorescence signals are captured and transformed for the image visualization [50]. They are both optical non-invasive techniques that permit *in vivo* and *ex vivo* (biopsy) images without the fixing, sectioning and staining, which are common procedures for histology analysis [54].

CLSM facilitates the image of living specimens, provides data from the three-dimensional structure of the sample and improves the image resolution due to high sensitivity, selectivity and versatility in fluorescent measures resulting in a valuable opportunity to study the behavior of pharmaceutical systems.

4. Advantages and disadvantages of using CLSM as a tool in skin delivery studies

Skin delivery research involves determination of physicochemical parameters of the formulation and *in vitro* and *in vivo* release studies. The fate of the drug/carrier into the living skin, either in healthy or pathological condition, is very important information; and CLSM can be a useful tool for development of cosmetic and dermatological products. The main advantages for studies with these aims include: (i) the ability to obtain images in a noninvasive manner *in vitro* and *in vivo* conditions [5]; (ii) suitable for *in vivo* diagnosis through imaging of superficial skin layers [49]; (iii) same skin site can be imaged serially over time that is an important advantage in studies like hair follicle neogenesis following wounding where the analysis are processed directly on the skin and information about number, length and width of follicles neogenics are obtained concurrently and from one animal [55]; (iv) ability to produce serial thin (0.5 to 1.5 μm) optical sections without mechanical sections and preserving the skin structure [5,16,47]; (v) eliminates artifacts that occur during physical sectioning and staining of sample; (vi) visualization of images at multiple depths through the sample without mechanical sections which allows the visualization of the skin layers where the drugs appropriately marked or dyes were able to achieve after their topical application [5,48]; (vii) ability in monitoring the skin penetration of drugs and delivery systems appropriately marked or dyes in real time, enabling, in this ways, bioavailability studies. This is done by performing analysis immediately after topical application of the dyes, for example, and after certain periods of time. Immediately after application, the dye was observed only in the stratum corneum, distributed in the intercellular spaces of the first layer of skin. In all other times analyzed; it is possible to assess whether the dye could penetrate the skin and if succeeded, the depth achieved [49]; (viii) high-resolution images; (ix) three-dimensional reconstruction from a series of optical sections at different depths; (x) sensitivity; (xi) versatility and selectivity florescence measures; (xii) reduced blurring of the image from light scattering and improved signal-to-noise that resulting in improvement of contrast and definition; (xiii) more precise quantification of images using image analysis software; (xiv) allows to analyze of fixed and live samples under a variety of conditions and with greater clarity [1,5,16,18,47-48].

However, the limitations of fluorophores and equipments as well as inherent interference of the tissue, bring some disadvantages of CLSM technique, such as: (i) limited number of excitation wavelengths available with common lasers; (ii) possibility to cause damage to living cells and tissues due to high intensity laser irradiation; (iii) autofluorescence of skin samples which may interfere in the analysis; (iv) problems in adjusting the focus on the skin surface due to cellular components and hydration state of the skin; (iv) limited special resolution that interfere significantly *in vivo* analyzes in dermatological practice where the maximum depth of analysis is around 200 μm, allowing diagnosis of only superficial skin disorders; (v) slow scanning laser action for high quality images; (vi) quantification in concentration terms since it is possible just when the relationship between probe and the fluorescence emission is linear and when this signal is not attenuated differently for each depth localization in the sample; (vii) high cost of acquisition and operation of systems for confocal microscopy [1,5,16,18,48,53].

5. CLSM technique for assessment of drug and delivery systems penetration into the skin and diagnosis of skin disorders

5.1. CLSM technique for assessment of drug and delivery systems penetration into the skin

CLSM is a valuable technique that helps to elucidate the mechanism, depth and distribution of skin penetration for delivery systems loaded or not with drugs. Nowadays, there is an increasing attempting to determine the possible penetration pathways because, with this information in hand, researchers are able to propose some structural modifications in the delivery systems, aiming to improve the skin penetration into the target tissue and, consequently, the pharmacological action of the drug [56]. Furthermore, penetration pathway elucidation is useful to address toxicological issue, since the fate of some formulations, mainly non-biodegradable nanoparticles, can be harmful to the body [44].

The emission of fluorescence by the delivery system and/or the drug is a condition when using CLSM for assessment of drug and delivery systems penetration into the skin. For that, the delivery systems are made fluorescent using probes covalently linked to polymers or homogeneously distributed in the system. In the case of the drugs, some studies link them to probes or, in many cases; they use a model probe with similar physicochemical properties of the drug. The mechanism of skin penetration from flexible polymerosomes, vesicles composed by polymers, was determined through the *in vitro* cutaneous penetration of vesicles containing Nile Red as the model probe. The skin samples were stained with fluorescein prior to fixation. The images (Figure 5) showed a time-dependence penetration into the skin, as initially, the particles tended to penetrate between the corneocytes isles (green stained) and, further application time, the vesicles tended to penetrate via intercellular lipids and follicular regions (red stained) until a maximum depth of 60 μm [57]. CSLM showed that a fluorescein loaded micelle formulation penetrate via follicular pathway and accumulate in epidermis up to a depth of 40 μm [34].

http://dx.doi.org/10.5772/55995

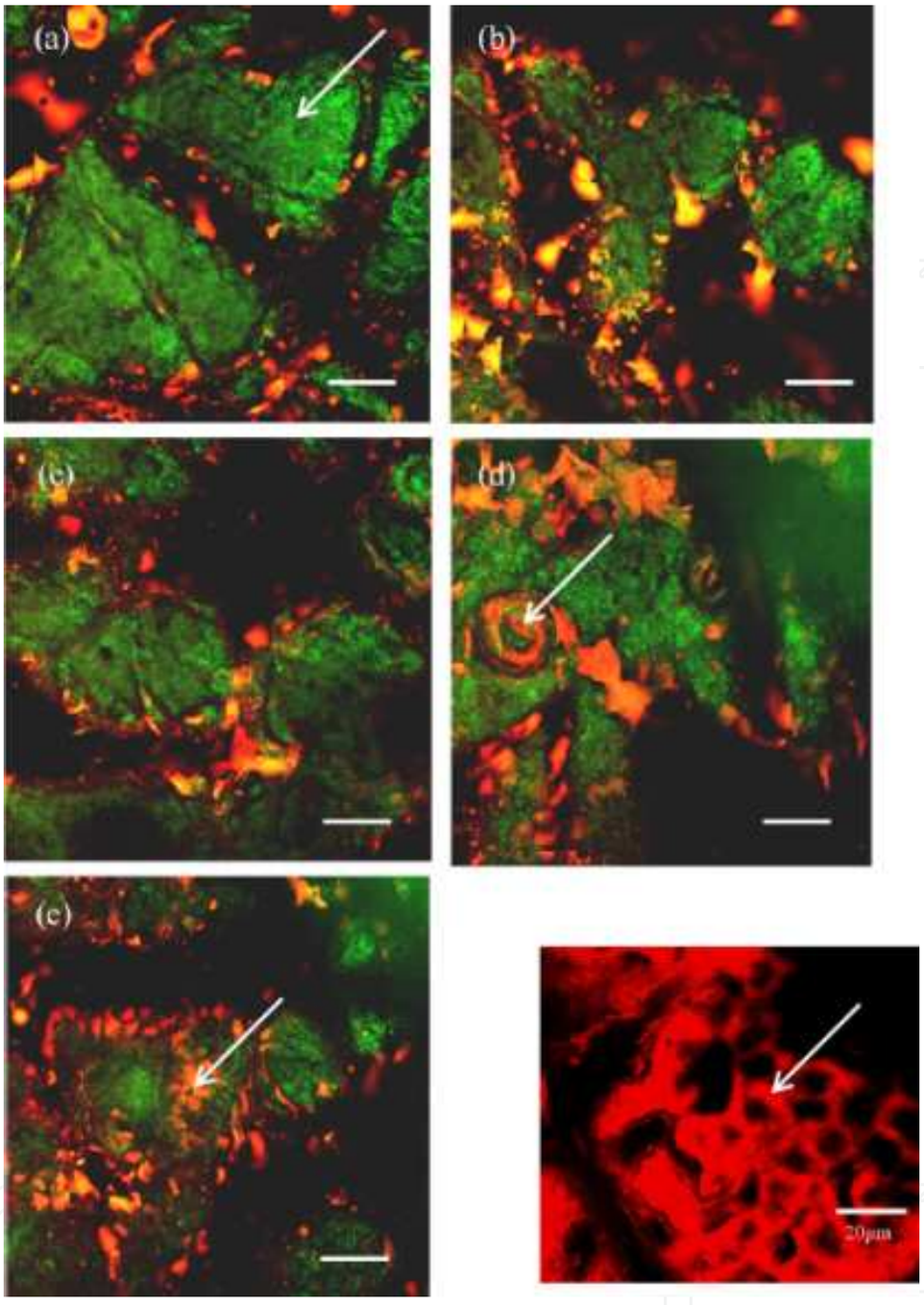

Figure 5. CLSM images showing distribution of polymer vesicles in cadaver epidermis with increasing durations: (a) 2 h, (b) 4 h, (c) 6 h, (d) 8 h and (e) 24 h. Inset depicts the accumulation of free Nile Red in the inter-corneocyte spaces. Being lipophilic in nature, the dye is seen to accumulate excessively in intercellular spaces (red stained). Vesicles initially (a) show localization in the 'furrows' between corneocyte groups (green stained) followed by the distribution in follicular (d) and intercellular spaces (e) (scale bar = 200 μm). Reproduced from [57] with permission.

It is possible to obtain CLSM images by sequential excitation using dual-labeled delivery systems, i.e., systems formulated with two different types of probes aiming to elucidate their mode of action. After *ex vivo* skin delivery, by sequential excitation of dual-labeled liposomes and vesicles carrying diclofenac, it was possible to show that the vesicles penetrated intact

down to the epidermis and the fluorescence intensity was higher and predominantly accumulated in the inter-corneocytes spaces [22]. Teixeira et al. (2010) [58], taking the advantage that the vitamin A (retinyl palmitate) fluoresces due to the presence of cromophore in its structure, obtained dual-labeled images after *in vitro* studies using elastic polymeric nanocapsules, marked with Nile blue, carrying the vitamin. The images (Figure 6) showed that the nanocapsule did not penetrate the skin carrying the vitamin, but a deep permeation (around 30 μm) of both was observed, which suggests that the drug present in deep skin layers was released from nanocapsules in the superficial skin layers. The uniform permeation of both labels suggests an intercellular permeation as the main mechanism for this type of nanocapsules. The visualization of dually labeled nanoparticles by the combination of multiphoton and CLSM in human skin biopsies showed that the polymeric nanoparticles did not penetrate the skin, whereas the dye Texas red, used to mimic a drug loaded in the nanoparticles, slowly penetrated the skin up to the stratum granulosum [59].

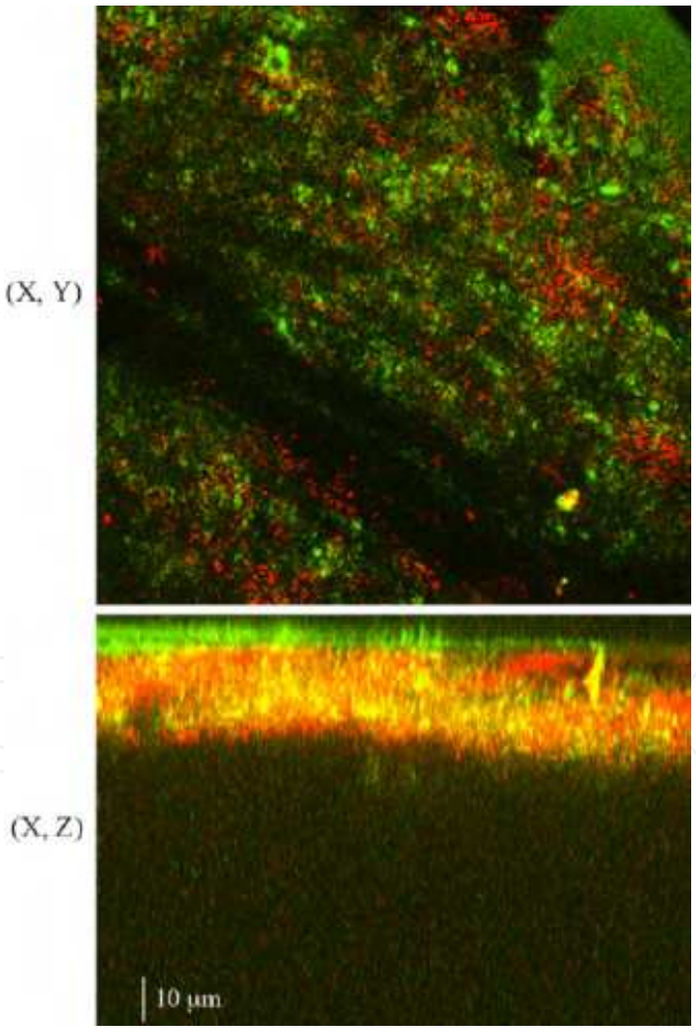

Figure 6. Confocal images of Nile blue-PLA nanocapsules. (a) xy image of the skin surface (initial fluorescence) and (b) deeper layers into skin, cross-sectional (xz mode) image. Red fluorescence, polymeric shell; green fluorescence, retinyl palmitate. Reproduced from [58] with permission.

http://dx.doi.org/10.5772/55995

Besides to determine the penetration in different skin layers, it is also possible to determine in which cellular site the drug preferentially penetrates. In this situation, Borowska et al. (2012) [35] stained skin sections with special dyes of high affinity to the nucleus before the *in vitro* skin penetration study using 8-MOP in formulations containing polyamidoamine dendrimers, conjugated with the probe fluorescein. CLSM images (Figure 7) revealed that 8-MOP encapsulated in dendrimers was able to penetrate into deep skin layers, epidermis and dermis, compared to standard formulation. In addition, the probe fluorescence (fluorescein) presented in the nucleus (blue stained) revealed that 8-MOP accumulated mostly in this cellular site important for its phototherapeutic activity.

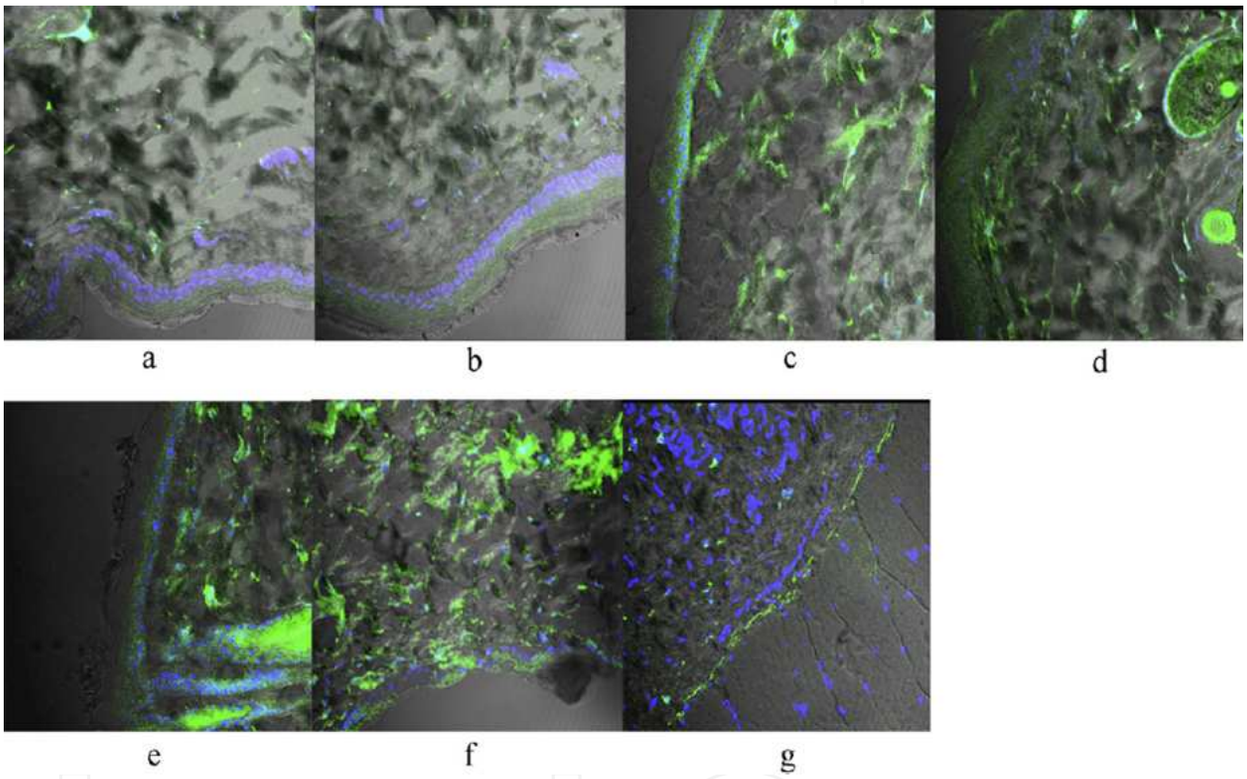

Figure 7. Distribution of 8-MOP (green) in rat's skin samples obtained by confocal microscopy following skin application of tested 8-MOP formulation. Cellular nuclei were counterstained with 7 AAD (blue): (a) 8-MOP after 1 h; (b) 8-MOP after 2 h; (c) 8-MOP-G3 PAMAM after 1 h; (d) 8-MOP-G3 PAMAM after 2 h; (e) 8-MOP-G4 PAMAM after 1 h; (f) 8-MOP-G4 PAMAM after 2 h; (g) 8-MOP-G4 PAMAM after 2 h – all skin layers and subcutaneous fatty tissue. Reproduced from [35] with permission.

In order to compare the skin penetration enhancement ability of different carriers and formulations, probes are visualized in the skin samples by CLSM after permeation studies. The fluorescence signal of a probe in liposome and transfersome containing valsartan was scanned at different skin depths after *in vitro* skin permeation studies. The results showed an increased skin penetration up to the dermis when valsartan was loaded in transfersomes, compared to rigid liposomes. The fluorescence liposomes was visualized up to 50 μm, while transfersomes were assessed up to 150 μm with a high fluorescence intensity and homogeneous skin distribution, evidencing the transdermal potential of transfersomes compared to liposomes [56]. CLSM

showed an improved and homogeneous skin penetration of the probe rhodamine B in the role epidermis using β- cyclodextrin composite ethosomal gel carrying the drug clotrimazole compared to gel and ethosomal gel formulations [60]. The *in vitro* percutaneous permeation of ethosomes, containing the drug 5- fluorouracil and labeled with rhodamine 6GO, in human hypertrophic scar and normal skin was assessed by CLSM. The images (Figure 8) showed a higher fluorescence intensity throughout the hypertrophic skin than normal skin compared to hydroethanolic solution, evidencing that the skin penetration of ethosomes was superior than the control in this type of skin [45]. Labeled (Nile red) solid lipid nanoparticles loaded with tacrolimus also showed improved skin penetration in various layers of skin (in the order of 5–6 times) compared to control, an ointment formulation [61].

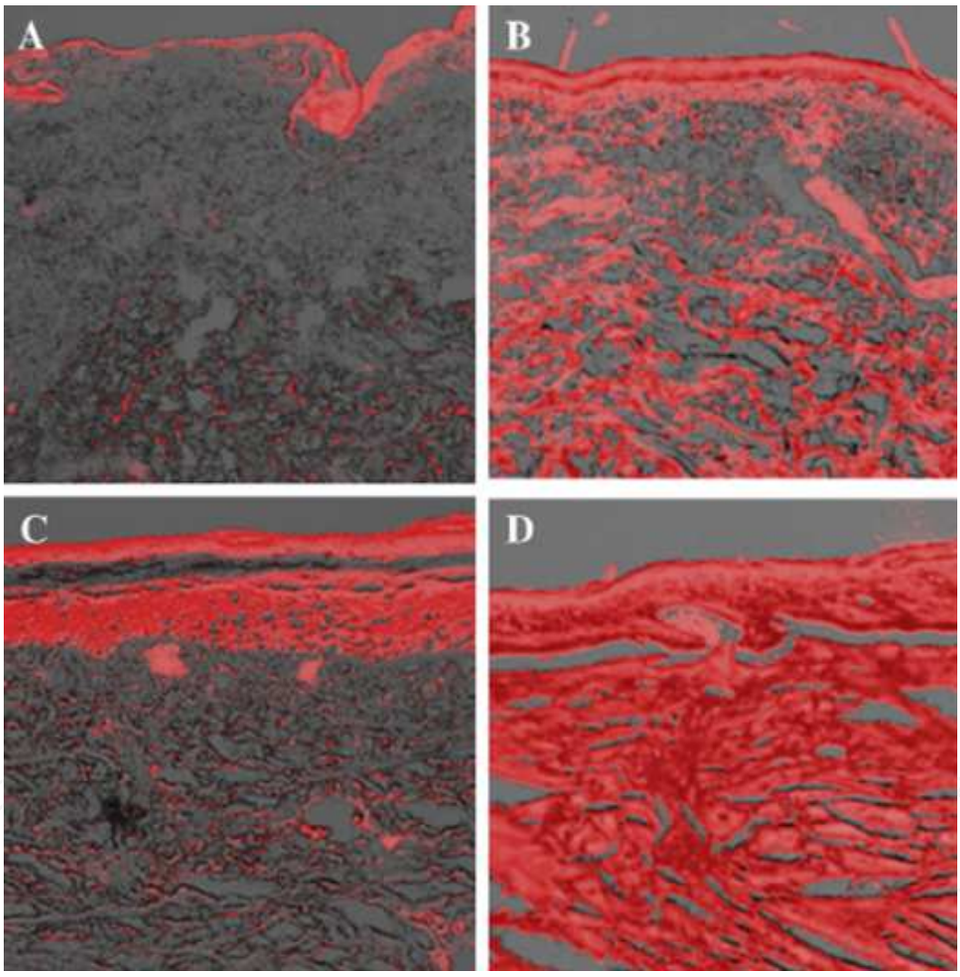

Figure 8. CLSM images of cross-sections of (A) human skin after application of rhodamine 6GO–hydroethanolic solution; (B) human skin after application of rhodamine 6GO–ethosomes; (C) human hypertrophic scar after application of rhodamine 6GO–hydroethanolic solution; and (D) human hypertrophic scar after application of rhodamine 6GO–ethosomes for 24 hours. Each image represents a 500 μm × 500 μm area. Reproduced from [45] with permission.

CLSM is extensively used to elucidate whether or not non-biodegradable nanoparticles penetrate the skin. Aiming to investigate the distribution of this type of nanoparticles (20 nm and 200 nm), covalently linked with FITC, across excised porcine skin, and to elucidate the

http://dx.doi.org/10.5772/55995

pathways of penetration into/through the cutaneous barrier, Alvarez-Roman et al. (2004) [62] obtained CSLM images showing that FITC-nanoparticles preferentially accumulated in the hair follicles and furrows that demarcate clusters of corneocytes (Figure 9). Furthermore, images from the xz plane showed that, independently of size, both nanoparticles did not penetrate the skin being localized at the furrows. Similar results were obtained by Campbell et al. (2012) [36] who verified polystyrene nanoparticles in the top layers of the stratum corneum up to a depth of 2-3 μm.

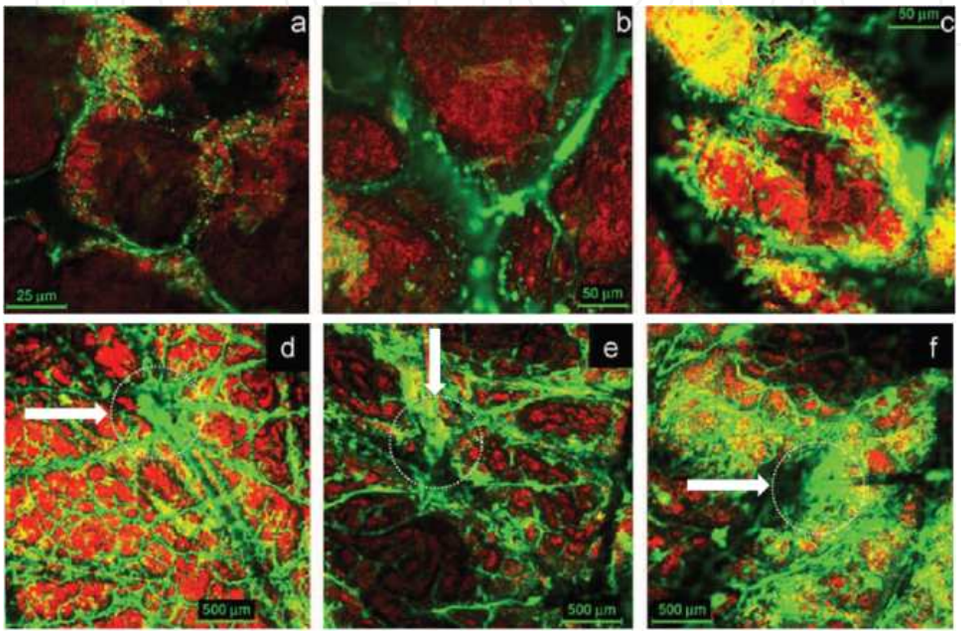

Figure 9. Dual label *x–y* images of the skin surface subsequent to treatment with FITC-nanoparticles (20 nm) for (a) 0 min, (b) 1 h, and (c) 2 h. The green fluorescence in figures a and c corresponds to furrows where nanoparticles accumulated. Follicular localization of FITC-nanoparticles subsequent to application of nanoparticles (200 nm) for (d) 30 min, (e) 1 h, and (f) 2 h. The white circles correspond to hair follicles. The red color corresponds from the fluorescence emanating from the porcine skin and the yellow-green from the FITC-nanoparticles. Reproduced from [62] with permission.

Photodynamic therapy studies take the advantage that the drugs (photosensitizers) used for cancer treatment self-fluoresce and CLSM technique is extensively used to assess the skin localization of the photosensitizer after *in vitro* topical application of a delivery system, once its skin penetration, besides other factors, is responsible for the success of the treatment. De Rosa et al. (2000, 2004) [9,63] verified by CLSM images (Figure 10) that the skin penetration and accumulation of protoporphyrin IX, an endogenously photosensitizer obtained from 5-aminolevulinic acid (5-ALA) by the biosynthetic pathway of heme, depended on the presence of penetration enhancer substance in the vehicle and 5-ALA derivative used. The presence of 5-ALA in ethosomes influenced the penetration depth and fluorescence intensity obtained from protoporphyrin IX after *in vivo* skin penetration [64]. CLSM also confirmed the improved biodistribution of a photosensitizer, zinc pthalocyanine tetrasulfonate, when using a microemulsion [10].

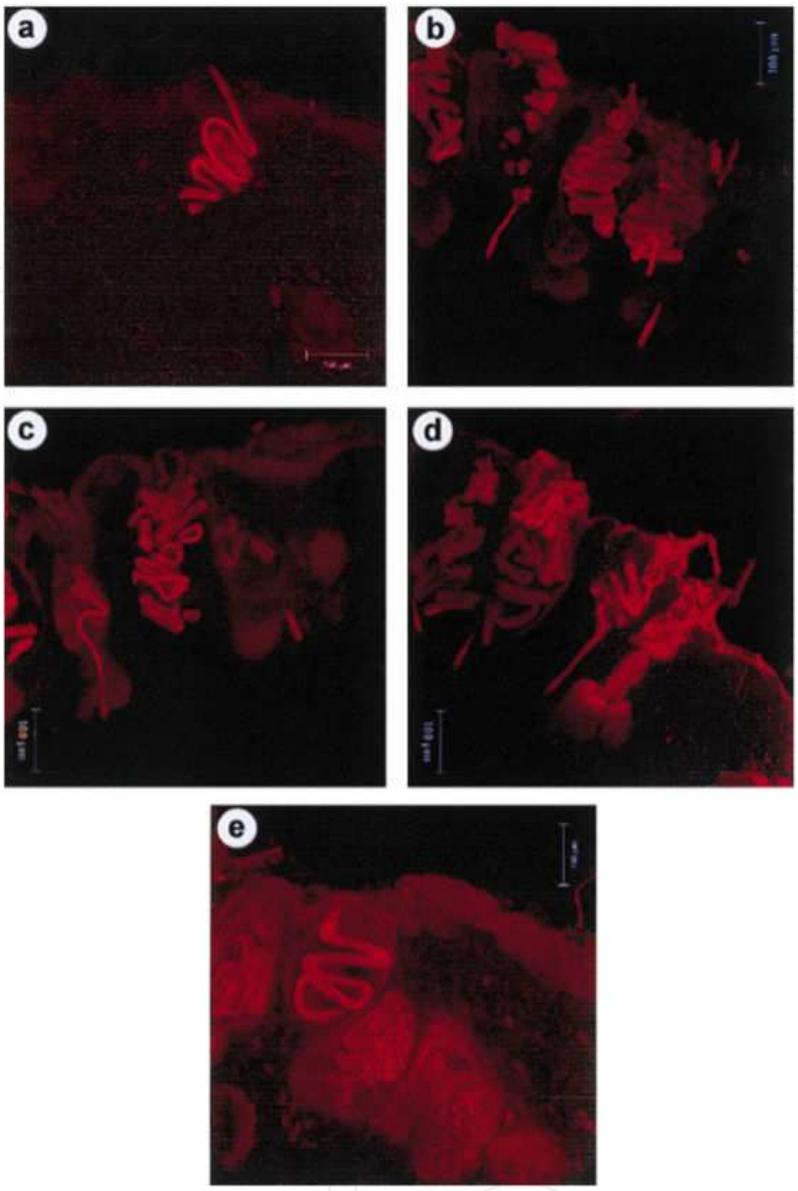

Figure 10. CLSM images of mechanical cross sections of hairless mouse skin (perpendicular series), optically sectioned 10 μm below the cutting surface: (a) control (untreated skin); skin treated with: (b) 10% 5-aminolevulinic acid (w/w); (c) 20% Dimethylsulphoxide (DMSO) (w/w); (d) 10% 5-aminolevulinic acid + 10% DMSO; and (e) 10% 5-aminolevulinic acid (w/w) + 20% Dimethylsulphoxide (w/w). All applied formulations contained 3% EDTA (w/w). Compared to controls (Figure 10 (a)), increases of red fluorescence in skins treated with 5-aminolevulinic acid (Figure 10 (b)), Dimethylsulphoxide (Figure 10 (c)), or with associations of these substances (Figures 10 (d) and 10 (e)), can be clearly seen as points with intense red fluorescence, indicating a PpIX accumulation. The association of 10% 5-aminolevulinic acid + 20% DMSO provided higher accumulation of PpIX, being considered more adequate for topical photodynamic therapy. Reproduced from [9] with permission.

CLSM is also used to assess the skin penetration of drugs after pre-treatment of the skin by physical methods, such as, sonophoresis, iontophoresis, microneedles and laser. Zhang et al. (2010) [27] showed that the pre-treatment of skin with microneedles permits the skin penetration of PLGA nanoparticles in the epidermis and dermis, and this would benefit a sustained drug release in the skin, supplying, in this way, the skin with drug over a prolonged period.

http://dx.doi.org/10.5772/55995

The depth of skin penetration from the drug heparin (FITC-labeled) was assessed *in vitro* in skins that were previously subjected to pretreatment using enhancement strategies by physical methods, such as sonophoresis, iontophoresis and microneedles. The study showed (Figure 11) that microneedles pretreatment was the only enhancement strategy that permitted heparin to reach the epidermis and deeper dermal layers, since FITC-labeled heparin was observed to follow microchannels formed by the microneedle device [65]. The influence of the low fluence fractional laser on the penetration of high molecular weight model drug, a polypeptide, FITC and FITC-labeled dextran (MWs of 4 and 150 kDa), was assayed by CSLM, whose image of skin showed a fluorescence increase in the upper and middle dermis, as well as in hair shafts and hair sheaths, evidencing a transfollicular route for high molecular weight substances [66].

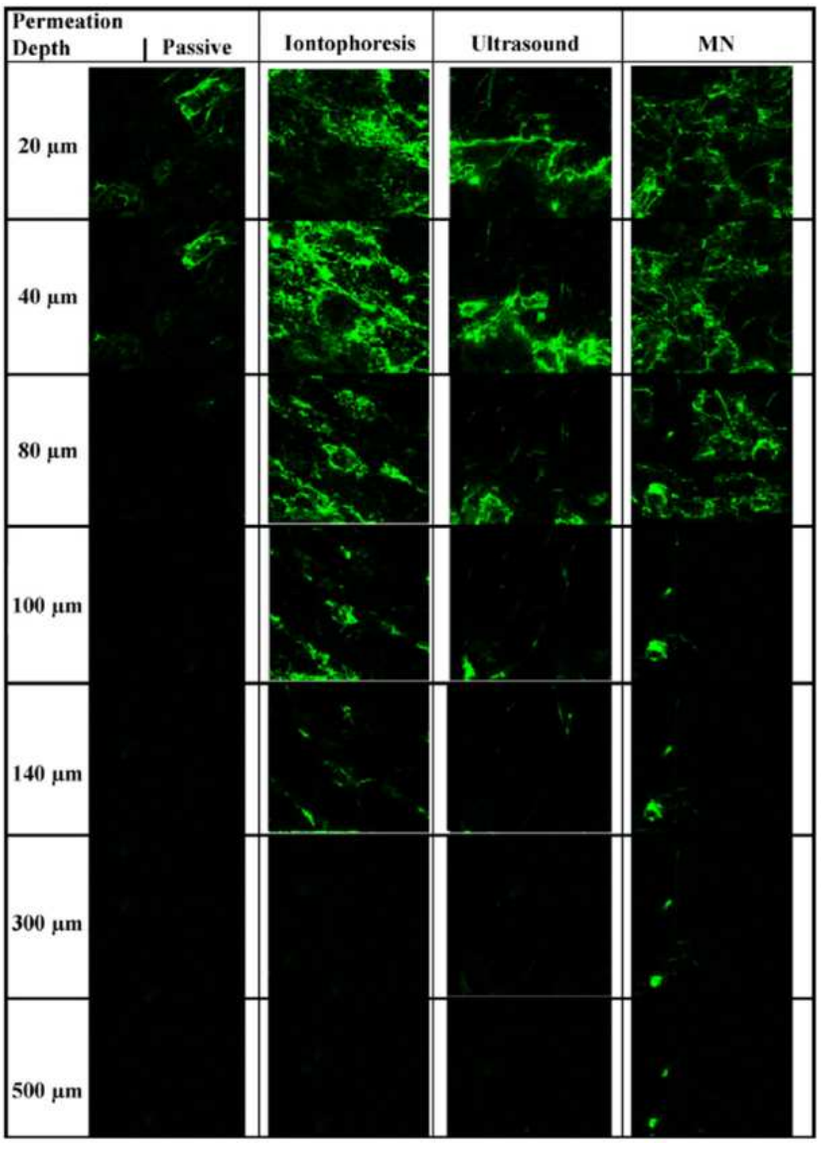

Figure 11. CLSM (X10 objective) of the permeation of FITC-labeled heparin across hairless rat skin at various depths from the surface of the stratum corneum. Heparin transported across microchannel can be seen as a florescent green color up to a depth of 500 µm. Reproduced from [65] with permission.

5.2. Non–invasive method for diagnosis of skin disorders and diseases

As mentioned before, CLSM can be used in fluorescence and reflectance modes for studies of skin disorders and diseases. It allows optical en face sectioning with quasihistological resolution and good contrast within living intact human tissue. The resolution allows for imaging of nuclear, cellular and tissue architecture of epidermis and the underlying structures, including connective tissue, inflammatory infiltrates, tumour cells, capillaries, and even circulating blood cells, without a biopsy [67].

Technically, confocal microscopes used in dermatology are not very different from their counterparts used in basic sciences. Typically, confocal microscopy employs lasers as sources of illumination due to their capability to generate monochromatic, coherent beams [54]. Confocal reflectance microscopy (CRM) in dermatology uses a near-infrared laser at 830 nm operating at a power of less than 20 mW, which is harmless for the tissue [67], whereas fluorescent confocal microscopes use He/Ne, Kr or Ar lasers to illuminate fluorescent samples in a wavelength range of 400-700 nm [68].

The company Lucid Inc. (Rochester, NY, USA) introduced in 1997 the first generation confocal microscope called VivaScope 1000. This microscope had a bulky configuration impeding convenient attachment to certain anatomical areas and imaging was very time consuming. The most widely used confocal microscope for imaging of human skin, the VivaScope 1500, was commercialized in the year 2000. This device is considerably smaller, more flexible and portable in contrast to its stationary predecessor. Further developments are the VivaScope 3000, a handheld confocal microscope for imaging of difficult to access areas, and the *ex vivo* VivaScope 2500 designed for imaging of excised tissue, especially in Mohs surgery as well as Vivascope 1500 Multilaser, which combines fluorescence laser scanning microscopy and confocal reflectance microscopy (CRM) modes [7].

In dermatology, CRM has several uses, such as: i) to diagnose diseases non-invasively *in vivo* [69-72]; ii) to non-invasive monitoring of treatment response *in vivo* and permits early detection of subclinical disease [73]; iii) to improve the accuracy of clinical diagnosis [74]; iv) to improve clinical discrimination between benign and malignant lesions [75]; v) to evaluate the same skin site over time because it produces no tissue damage [76]; vi) to assess the boundaries of the lesion pre- or post-surgery [54]; vii) to evaluate the dynamics of structural and cellular changes that take place during the occurrence of the disease [77]; and viii) to study physiopathologic processes non-invasively over time [78-79].

Despite the benefits, CRM has some limitations, such as: i) not all lesions image well; ii) subject motion occurs frequently; iii) the depth of imaging is limited at present to only 200 to 500 μm (epidermis and superficial dermis); iv) the presence of refractive structures may also decrease contrast and make melanocyte visualization difficult; v) lesions with a thick epidermis or certain anatomic sites, such as the palm or sole, will image very superficially; vi) images are viewed in horizontal sections rather than vertical sections (as in conventional histopathology), which makes direct comparisons difficult and requires experience to properly interpret images [67,74]; and vii) the relative high cost of CRM (approximately $50,000). Although the upfront cost of the device is high, the supplies to image individual lesions cost only about $1 per lesion, allowing imaging of multiple lesions with minimal increased cost to the patient per lesion [80].

http://dx.doi.org/10.5772/55995

Recently, there was a formation of an international CRM group (www.skinconfocalmicroscopy.org) constituted by clinicians who use this technique for diagnosis and monitoring, researchers and experts in many aspects of CRM to dermatology. By providing a forum for free communication of results, the establishment of meaningful collaborations and formation of trained personnel, this group aims to spread the use of CRM in dermatology [54].

5.2.1. CRM to diagnose melanocytic lesions

Langley et al., in 2001 [74], were the first to publish a study of benign and malignant melanocytic lesions by *in vivo* confocal microscopy. In the study, they discovered apparent differences in the CRM characteristics of nevi, dysplastic nevi, and melanomas (Figure 12), indicating that this tool could be helpful in the clinical discrimination of benign and malignant melanocytic lesions. The diagnostic applicability of CRM in melanocytic skin tumours, determined by evaluating sensitivity, specificity, positive and negative predictive value was first described by Gerger et al. in 2005 [81]. In 2006, Langley et al [75] determined that CRM has sensitivity and specificity compared to dermoscopy for the diagnosis of melanoma.

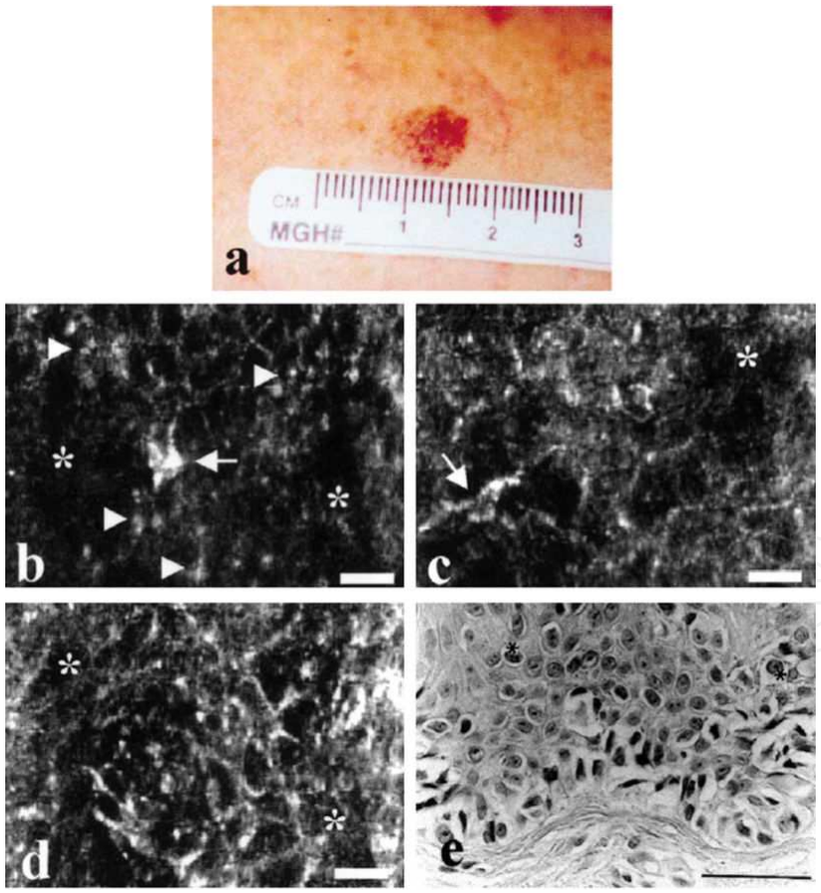

Figure 12. Clinical photograph of superficial spreading melanoma, invasive to anatomic level II, with a measured depth of 0.44 mm on the right posterior shoulder of 47-year-old man. This lesion was clinically diagnosed as dysplastic nevus, but by CLSM showed features consistent with melanoma. b-d, Confocal images of melanomas. Key features noted in melanomas as viewed by CLSM were loss of keratinocyte cell border (asterisks in B-D); bright, granular, highly

refractile particles (arrowheads in b); and atypical stellate cells (arrows in b and c). Scale bar = 25 µm. e, Histological section of intraepidermal component of superficial spreading malignant melanoma showing confluence of tumor cells at dermoepidermal junction as well as individual cells of varying levels of the epidermis, so-called "pagetoid" spread (asterisks). Scale bar = 50 µm. Reproduced from [74] with permission.

Benign nevi can be differentiated from melanomas by CRM and criteria proved to be valuable [81-84]. CRM features can distinguish lentigo maligna (Figure 13) from benign macules of the face such as solar lentigo, ephelis, actinic keratosis, and flat seborrheic keratosis [70,75,85].

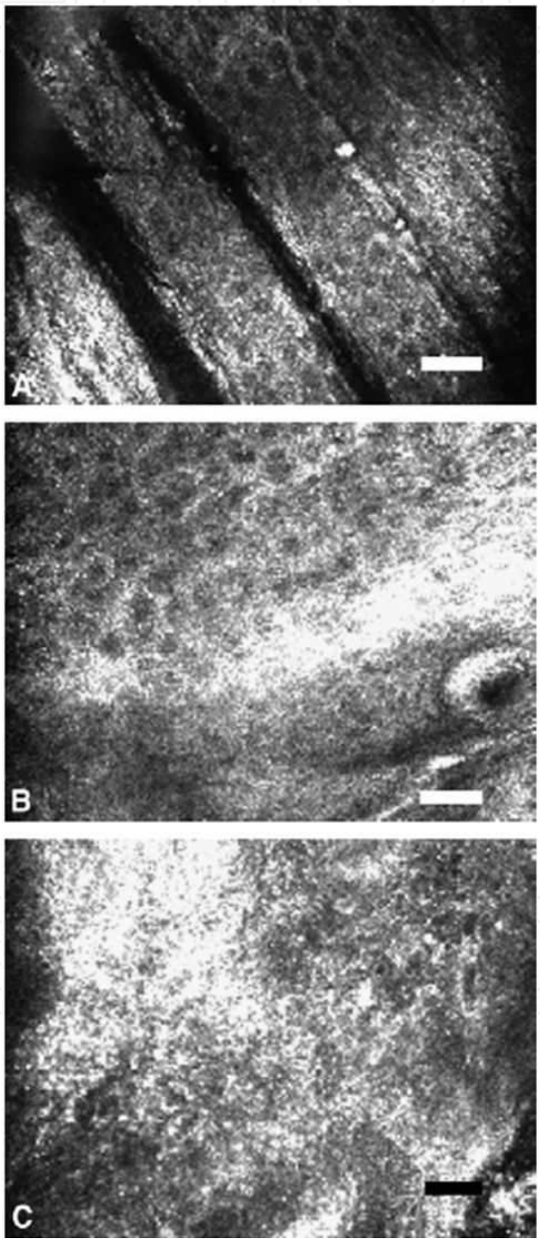

Figure 13. A, CRM image of control skin at the stratum spinosum displaying well-organized keratinocyte cell borders. B, CRM image of lentigo at the level of the stratum spinosum. The well-organized honey combed pattern of keratinocyte cell borders is preserved. C, CRM image of lentigo maligna at the stratum spinosum level. There is loss of keratinocyte cell borders, and a grainy image is noted. (Scale bar, 50 µm.). Reproduced from [75] with permission.

http://dx.doi.org/10.5772/55995

Even non-melanotic lesions can be recognized by CRM because of the presence of melanosomes and melanin granules in their cytoplasm [70,86-87].

5.2.2. CRM and non–melanocitic lesions

The clinical diagnosis of actinic keratosis by CRM (Figure 14) was first determined by Aghassi et al. (2000) [78]. Later, others confirmed the usefulness of this tool [73,88-89], although it has not been able to unequivocally differentiate actinic keratosis from squamous cell carcinomas [90].

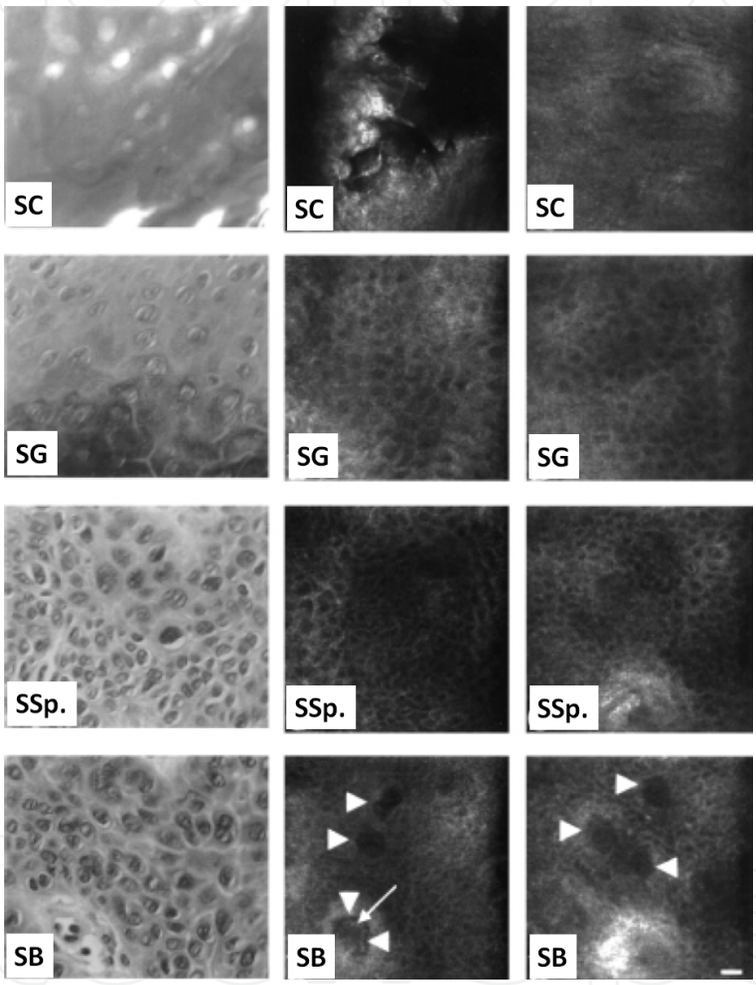

Figure 14. Left column is conventional histopathology of actinic keratosis (AK), center is CRM of AK, and right column is CRM of adjacent normal skin. Sections were obtained by means of conventional histopathology of AK (hematoxylin-eosin stain; original magnification ×20; 0.4 numerical aperture, dry objective lens), CM of AK (×30, 0.9 numerical aperture, water immersion objective lens, scale bar = 25 μm),and CM of adjacent normal skin (original magnification ×30, 0.9 numerical aperture, water immersion objective lens, scale bar = 25 μm). SC, Stratum corneum. Irregular hyperkeratosis of AK is evident on conventional histopathology and CRM, contrasting with smooth surface of normal skin. SG, Stratum granulosum. Conventional histopathology and CRM demonstrate uniform, evenly spaced, broad keratinocytes both in AK and normal skin. In CRM images, nuclei appear dark in contrast to bright, refractile cytoplasm. SSp., Stratum spinosum. Conventional histopathology and CRM of AK show enlarged, pleomorphicnuclei with haphazard orientation, contrasting with small, uniform, evenly spaced nuclei from normal skin. SB, Stratum basale. Conventional histopathology and CRM of AK show enlarged, pleomorphic nuclei with haphazard orientation, contrasting with small, uniform, evenly spaced nuclei from normal skin. In CRM images, dermal papillae appear as well-demarcated, dark holes in epidermis (arrowheads), containing blood vessels (arrow). Reproduced from [78] with permission.

CRM offers a sensitive and specific tool for the noninvasive diagnosis of basal cell carcinoma *in vivo* (Figure 15) [69,91-92] showing good correlation with histology.

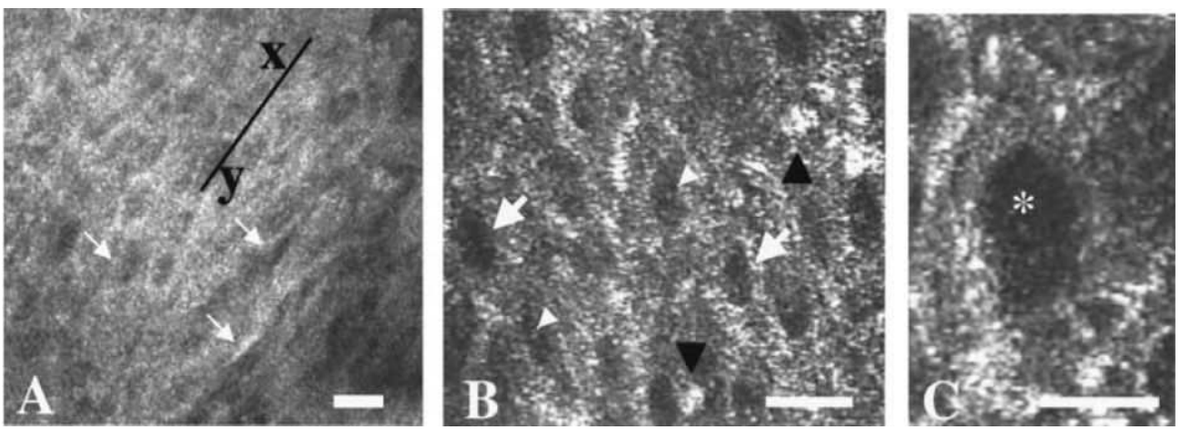

Figure 15. Real-time *in vivo* confocal images of a basal cell carcinoma (BCC) showing a uniform population of elongated cells (arrows, A and B) oriented along the same principal axis (x-y). Mononuclear cells (black arrowheads, B) are seen intermixed with BCC cells (arrows, B) with some of the BCC cells showing nucleoli (white arrowheads, B). C, High-power magnification of one BCC cell demonstrating a large elongated nucleus with a low refractility (asterisk), surrounded by a bright cytoplasm. (A-C, Hematoxylin-eosin stain; original magnifications: A, x30, 0.9 numerical aperture (NA) water-immersion objective lens; B and C, x100, 1.2 NA water-immersion objective lens. Scale bar, 25 μm). Reproduced from [91] with permission.

Non-melanoma skin cancers (NMSC) were evaluated by fluorescence confocal microscopy aiming to diagnose and monitor the lesions in reference to normal skin and correlation with routine histology. The results suggest that fluorescence confocal microscopy may allow a systematic, noninvasive histomorphometric evaluation of actinic keratosis and basal cell carcinoma, potentially aiding in the detection of subclinical actinic keratosis and early therapeutic management [93]. CRM was also evaluated to diagnose NMSC early and the authors concluded that *in vivo* CRM is a promising and innovative technology for the early diagnosis of skin cancer, which may ultimately play an important role in skin cancer screening and prevention as well as in the early detection of progression or recurrence after therapy [94].

5.2.3. CRM and other skin diseases

In vivo CRM resolves changes at the cellular and subcellular level comparable to that obtained with standard histology. In this case, this tool was successfully used to evaluate the dynamics of structural and cellular changes that take place during the occurrence of allergic contact dermatitis [77]. Furthermore, it is a promising tool for dynamic, noninvasive assessment and may help to differentiate acute and induced contact dermatitis (Figure 16) [76,79].

http://dx.doi.org/10.5772/55995

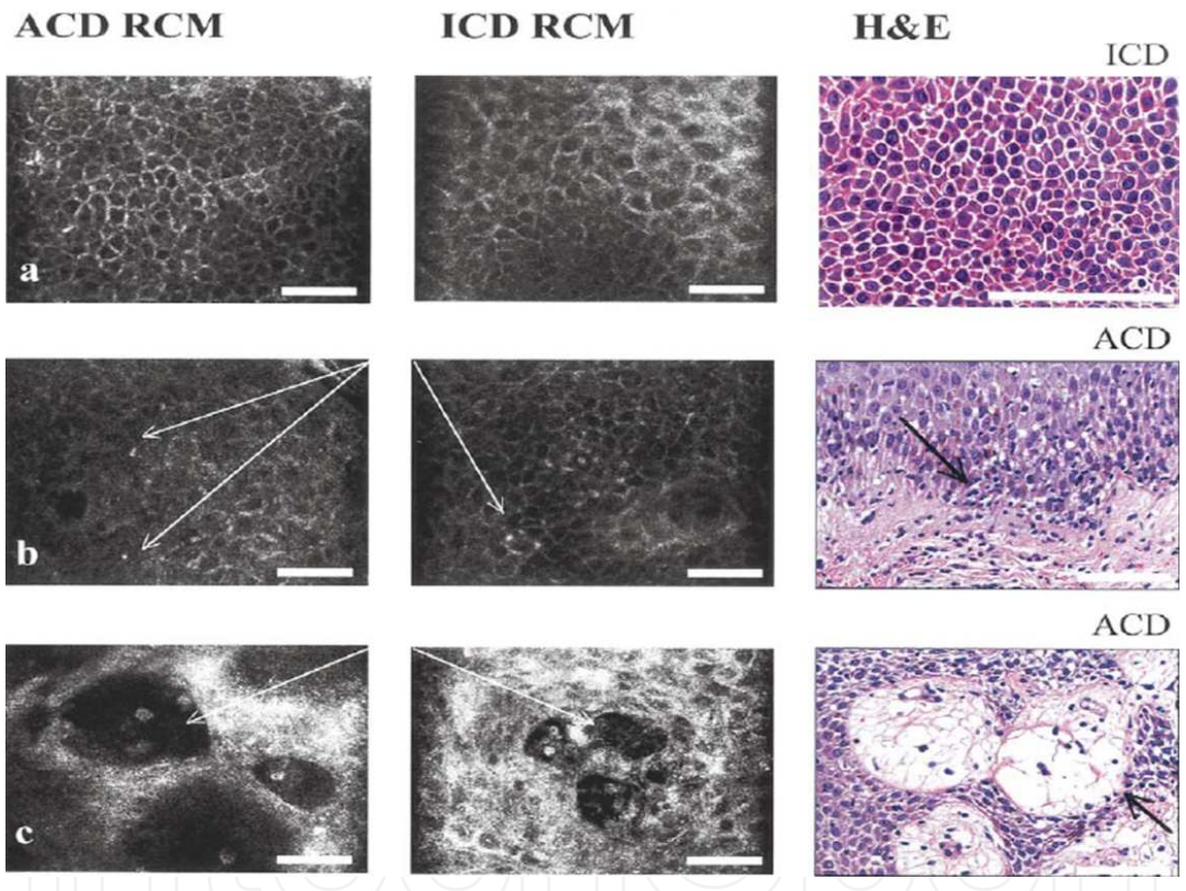

Figure 16. Features common to allergic contact dermatitis and irritant contact dermatitis observed with reflectance confocal microscopy CRM and correlated by routine histology. a, Spongiosis: increased intercellular brightness apparent on CRM. b, Inflammatory cell infiltrate: bright structures 12- to 15-μm size interspersed between keratinocytes. Arrows denote inflammatory cells. c, Intraepidermal vesicle (arrow) formation: dark spaces in epidermis containing inflammatory cells and necrotic keratinocytes. Scale bars = 50 μm. H&E, hematoxylin-eosin stain. Reproduced from [76] with permission.

CRM was also used to investigate lesions of progressive macular hypomelanosis (Figure 17) showing that the ''pigmented ring'' is intact, but its melanin content is decreased compared with the surrounding normal skin [95].

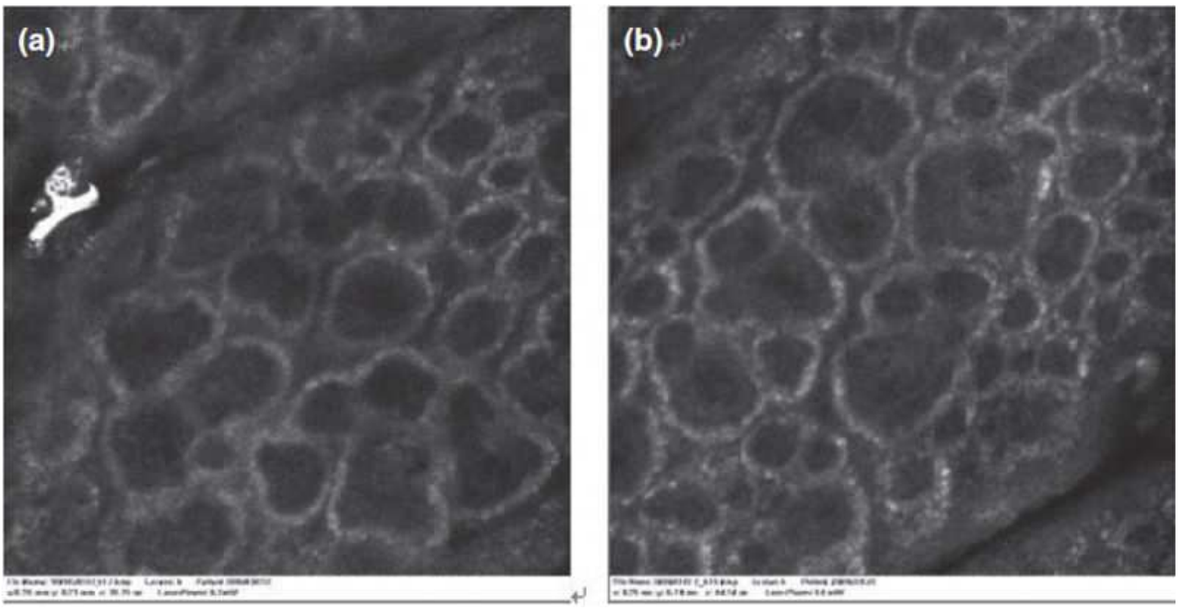

Figure 17. a) Lesion areas and (b) perilesional normal skin were observed under CRM. The ''pigmented ring'' around dermal papilla show completed, but compared with the surrounding normal skin its melanin content was decreased (the same horizon). Reproduced from [95] with permission.

Chiavèrini et al., 2001 [96] have shown crystalline deposits of cystine within the papillary dermis (Figure 18) by *in vivo* CRM, in patients with infantile cystinosis. The study concluded that CRM scoring of dermal cystine deposition could be used as a marker of treatment response complementary to the leukocyte cystine level.

CRM is a valuable tool to evaluate histological features of psoriasis (Figure 18), and the findings correlate with histology [97-99].

CRM imaging elucidates and monitors the dynamic pathophysiologic response, such as those that occur subsequent to laser treatment of cutaneous lesions, like cherry angiomas [78] and sebaceous gland hyperplasia [100-101]. Moreover, it facilitates the discrimination of sebaceous hyperplasia from basal cell carcinoma *in vivo* [102].

Noninvasive diagnosis of pemphigus foliaceus by CRM was consistent with the routine histology of the preexisting lesions [52] and criteria for diagnosing pemphigus (Figure 20) was established [72].

Diagnostic CRM criterion for mycosis fungoids was first determined by Agero et al. in 2007 [103] and later on confirmed by Lange-Asschenfeldt et al. (2012) [104].

Others diseases diagnosed by CRM *in vivo* were: discoid lupus erythematosus [105]; dermatophyte infections [106-108]; lichen sclerosus [109] and folliculitis [110].

http://dx.doi.org/10.5772/55995

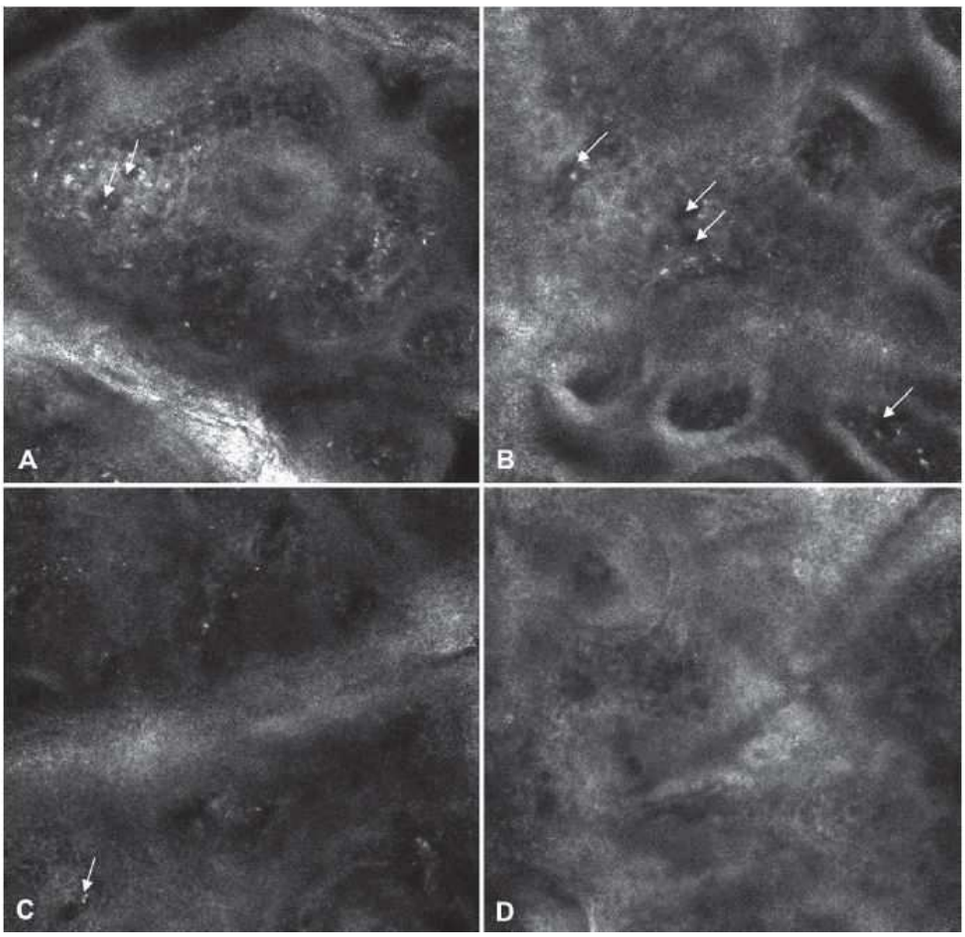

Figure 18. *In vivo* CRM of skin in infantile cystinosis. Confocal images of skin: block image of 4 x 4 mm. Numerous (+++) (A), few (++) (B), and some (+) (C) bright particles were seen around or in vessels (arrows) at level of dermis, in patients with cystinosis compared with control subjects (D). Reproduced from [96] with permission.

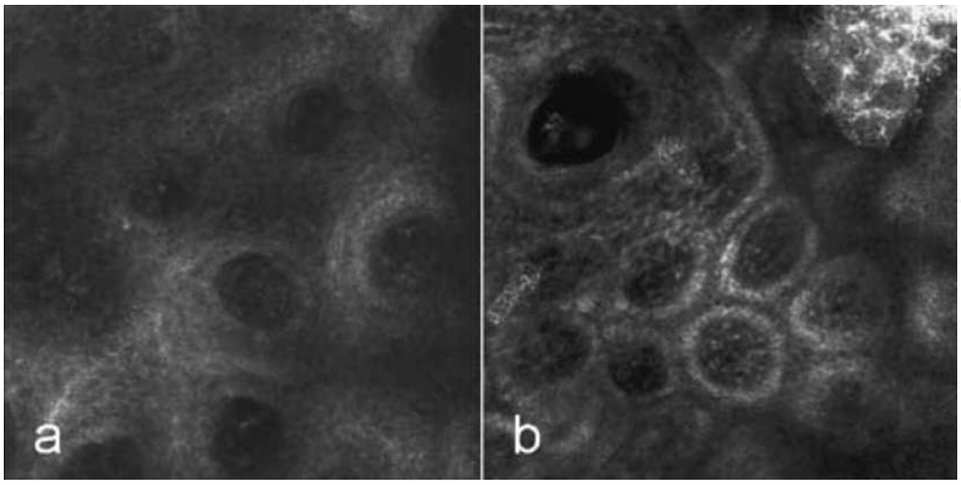

Figure 19. CRM image (0.5 × 0.5 mm) of the basal layer: absence of papillary rings in plaque psoriasis skin (a), compared to normal skin taken on symmetrical anatomical sites (b). Reproduced from [98] with permission.

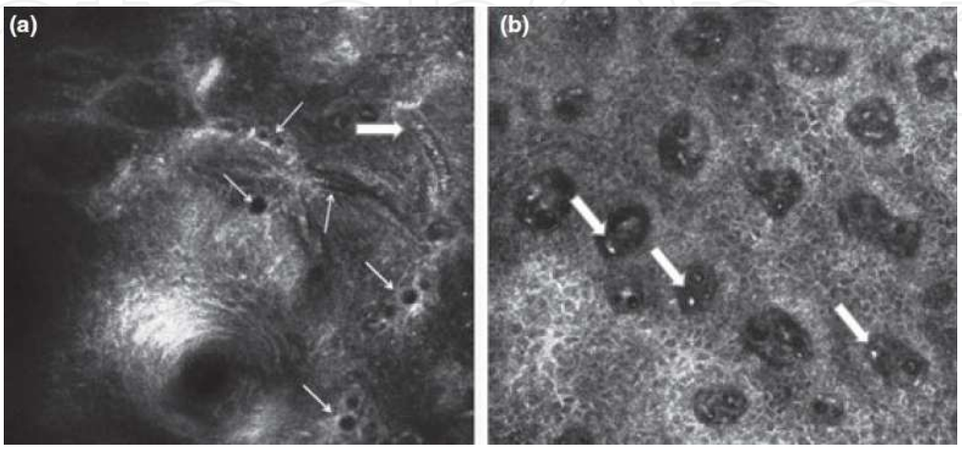

Figure 20. Dilated blood vessels (thin arrows) containing highly refractive peripheral blood cells (thick arrows) in pemphigus vulgaris (a) and pemphigus foliaceous (b) (0.5 x 0.5 mm). Reproduced from [72] with permission.

6. Pathways involved in penetration of drugs and biomolecules in the skin

The SC is the outmost layer of the skin and provides an efficient barrier for the ingress of extraneous substances and egress of endogenous substances [111]. The packing of the lipids (ceramides, cholesterol and free fatty acids) present in the SC are responsible for this barrier as they are arranged surrounding the corneocytes forming a "brick and mortar" model with the corneocytes as the bricks and the lipids as the mortar [112].

Drugs and biomolecules can penetrate the skin to the viable tissue by three main routes: i) the intercellular (between the corneocytes, through the lipid matrix); ii) the transcellular (through the corneocytes); and iii) the shunt (through the skin appendages, like hair follicles, sweat ducts and sebaceous glands). Generally, the intercellular pathway is predominantly for most molecules, and the shunt pathway is important for polymers and colloidal nanoparticles and large polar molecules [15].

CLSM helps to elucidate not only the extension and depth of skin penetration of drugs and biomolecules [10,45] but also the main pathways involved in their penetration. In this sense, the use of CLSM with other physicochemical techniques such as Raman [113], infrared spectroscopy [39], differential scanning calorimetry and small- and wide-angle X-ray scatter-

http://dx.doi.org/10.5772/55995

ing [114], occlusive studies [115], dermatopharmacokinetic analysis [39] and transmission electron microscopy [116], help to further elucidate the exact drug/skin interaction, i.e., the mechanism of skin penetration. In addition, these techniques also permit to determine the skin interaction of delivery systems [34,117-120] and the skin modification promoted by physical methods [32,121-123], aiding to clarify the exact mechanism by which these techniques increase the skin penetration of drugs and biomolecules.

Interesting study was carried out with microemulsion containing Nile red dye, showing that this delivery systems lead to a dye accumulation between the coneocytes of the role stratum corneum, evidencing an intercellular penetration route (Figure 21). Moreover, to address whether the microemulsion penetrated the stratum corneum or not, a dermatopharmacokinetic analysis of the microemulsion components across this skin layer helped to clarify that every component diffuses separately [39].

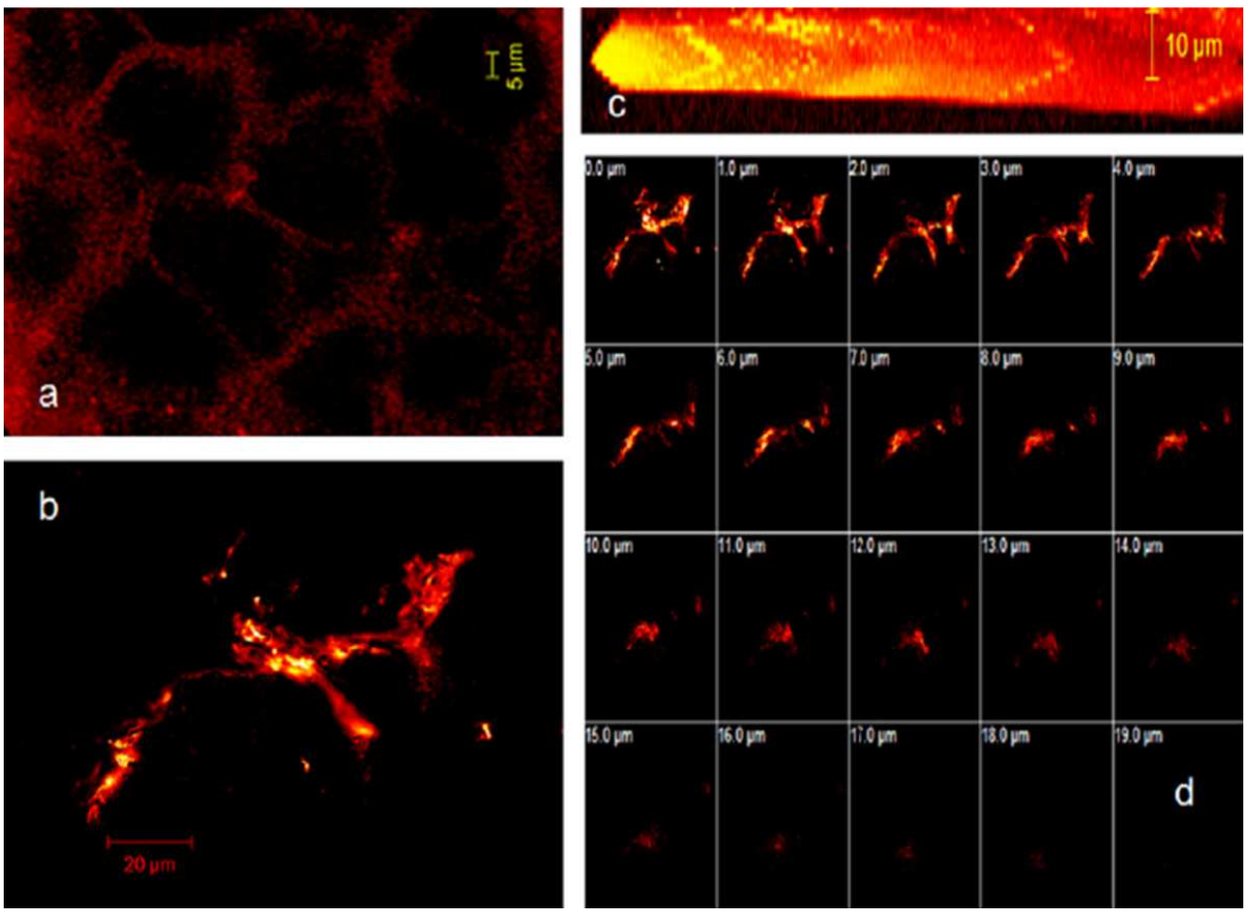

Figure 21. CLSM images of the microemulsion fluorolabelled with Nile red (a) and (b) Normal xy images, (c) Reconstructed xz image after sectioning through z-plane using one projection at 0º angle (sectioned from 0 to 20 µm with 1 µm increments) and (d) z-stack image. Reproduced from [39] with permission.

Table 3 shows the main skin permeation pathways uncovered by CLSM studies using different delivery systems, probes and methods of application.

Main Permeation Pathways	Delivery system/probe	Mechanism of skin application	Reference
Follicular	Ethosomes/β-carotene	Passive delivery	[117]
	Micelle/Fluorescein	Passive delivery	[34]
	Polystyrene nanoparticles/FITC	Passive delivery	[62]
	Nanoparticles/5-fluoresceinamine	Passive delivery	[118]
	Polypeptide, FITC and FITC-labeled dextran	Skin pre-treatment with fractional laser	[66]
Intercellular (lipid pathway)	Liposomes/fluorescein–DHPE	Passive delivery	[119]
	Ethosomes/Bacitracin-FITC	Passive delivery	[120]
	Posintro™ nanoparticles/Acridine	Passive delivery	[116]
	Elastic polymeric nanocapsules/ retinyl palmitate	Passive delivery	[58]
	Biphasic vesicles/Alexa 594-labeled Interferon α	Passive delivery	[114]
	Vesicles/β-carotene and carboxyfluorescein	Passive delivery	[22]
	Microemulsion/Nile red	Passive delivery	[39]
Transcellular (corneocytes pathway)	FITC label oligonucleotide	Electroporation	[121]
Mixed Inter and Transcellular	Calcein dissolved in phosphate buffer	Iontophoresis and high voltage pulsing	[122]
	Fluorescein isothiocyanate dextran dissolved in phosphate buffer	Low-frequency sonophoresis	[32]
Channels in the stratum corneum	Elastic liposomes/Rhodamine red	Passive delivery	[124]
Lacunar regions of the intercellular lipids and follicular	Quantum dots (cationic, neutral and anionic)	Ultrasound and sodium lauryl sulphate	[44]
Intercellular and follicular	Flexible polymerosomes/Nile red	Passive delivery	[57]

Table 3. Skin permeation pathways uncovered by CLSM studies

7. Future perspectives

The use of confocal microscopy in recent years has revolutionized many aspects in the pharmaceutical and medical sciences. It is an useful tool that aids to develop and improve delivery systems aimed to reach certain targets in the skin; it permits to elucidate the mechanisms of penetration of these systems in relevant skin models and to uncover the cellular

uptake of drugs; and help to diagnose cutaneous pathologies. The ability to obtain non-invasively images with high resolution and sensitivity, at different depths of the sample and three-dimensional reconstruction are important advantages of this technique. The assessment of various delivery systems *in vitro* by CLSM provides a better characterization of their physicochemical properties and their behavior and the ability to view them *ex vivo* and *in vivo* allows us to elucidate their mechanisms *in situ*. With this, the rational development of topical delivery systems becomes more effective.

The use of CLSM in the reflectance mode to diagnose skin disorders is relatively recent and the challenge in this area is related to the presence of substantial clinical studies that compares morphological confocal features with histology and establishes their correlations, the formation of trained and experienced personnel and the cost of the equipment. Although its usefulness related to the collection of images fast and relatively ease, some limitations of the technique related to the equipment capability still limits its wide use in dermatology.

In this context, improvements in equipment, fluorescent probes and confocal microscopy techniques will enhance and promote new opportunities for studies involving skin, cosmetic and pharmaceutical products, since it is clear the important contribution of CLSM in this application area.

Author details

Fábia Cristina Rossetti, Lívia Vieira Depieri and Maria Vitória Lopes Badra Bentley*

*Address all correspondence to: vbentley@usp.br

Faculdade de Ciências Farmacêuticas de Ribeirão Preto, Universidade de São Paulo, Avenida do Café, s/n, Ribeirão Preto, SP, Brazil

References

[1] Pygall, S. R, Whetstone, J, Timmins, P, & Melia, C. D. Pharmaceutical applications of confocal laser scanning microscopy: The physical characterisation of pharmaceutical systems. Advanced Drug Delivery Reviews (2007).

[2] White, P. J, Fogarty, R. D, Liepe, I. J, Delaney, P. M, Werther, G. A, & Wraight, C. J. Live confocal microscopy of oligonucleotide uptake by keratinocytes in human skin grafts on nude mice. Journal of Investigative Dermatology (1999).

[3] Ghartey-tagoe, E. B, Morgan, J. S, Ahmed, K, Neish, A. S, & Prausnitz, M. R. Electroporation-mediated delivery of molecules to model intestinal epithelia. International Journal of Pharmaceutics (2004).

[4] Verma, D. D, Verma, S, Blume, G, & Fahr, A. Liposomes increase skin penetration of entrapped and non-entrapped hydrophilic substances into human skin: a skin penetration and confocal laser scanning microscopy study. European Journal of Pharmaceutics and Biopharmaceutics (2003).

[5] Alvarez-román, R, Naik, A, Kalia, Y. N, Fessia, H, & Guy, R. H. Visualization of skin penetration using confocal laser scanning microscopy. European Journal of Pharmaceutics and Biopharmaceutics (2004).

[6] Brus, C, Santi, P, Colombo, P, & Kissel, T. Distribution and quantification of polyethylenimine oligodeoxynucleotide complexes in human skin after iontophoretic delivery using confocal scanning laser microscopy. Journal of Controlled Release (2002).

[7] Hofmann-wellenhof, R, Pellacani, G, Malvehy, J, & Soyer, H. P. editors. Reflectance Confocal Microscopy for Skin Diseases. Springer-Verlag Berlin Heidelberg; (2012).

[8] Cullander, C. The laser-scanning confocal microscope. In: Wilhelm K-P., Elsner P., Berardesca E., Maibach HI. (eds.) Bioengineering of the Skin: Skin Surface and Analysis. CRC Press, Boca Raton; (1997). , 23-37.

[9] De Rosa, F. S, Marchetti, J. M, Thomazini, J. A, & Tedesco, A. C. Bentley MVLB. A vehicle for photodynamic therapy of skin cancer: influence of dimethylsulphoxide on aminolevulinic acid *in vitro* cutaneous permeation and *in vivo* protoporphyrin IX accumulation determined by confocal microscopy. Journal of Controlled Release (2000). , 5.

[10] Rossetti, F. C, Lopes, L. B, Carollo, A. R, Thomazini, J. A, & Tedesco, A. C. Bentley MVLB. A delivery system to avoid self-aggregation and to improve *in vitro* and *in vivo* skin delivery of a phthalocyanine derivative used in the photodynamic therapy. Journal of Controlled Release (2011).

[11] Menon, G. New insights into skin structure: scratching the surface. Advanced Drug Delivery Review (2002). SS17., 3.

[12] Foldvari, M. Non-invasive administration of drugs through the skin: challenges in delivery system design. Pharmaceutical Science & Technology Today (2000).

[13] Kendall, A. C, & Nicolaou, A. Bioactive lipid mediators in skin inflammation and immunity. Progress in Lipid Research (2013).

[14] Elias, P. M, & Friend, D. S. The permeability of the skin. Physiological Reviews (1971).

[15] Barry, B. W. Novel mechanisms and devices to enable successful transdermal drug delivery. European Journal of Pharmaceutical Sciences (2001).

[16] Verma, D. D, & Fahr, A. Confocal Laser Scanning Microscopy: An Excellent Tool for Tracking Compounds in the Skin. In: Smith WE., Maibach HI. (ed.) Percutaneous Penetration Enhancers. Taylor & Francis Group; (2006). , 335-357.

[17] Paddock, S. W. Principles and Practices of Laser Scanning Confocal Microscopy. Molecular Biotechnology (2000).

[18] Meng, F, Liao, B, Liang, S, Yang, F, Zhang, H, & Songe, L. Morphological visualization, componential characterization and microbiological identification of membrane fouling in membrane bioreactors (MBRs). Journal of Membrane Science (2010).

[19] Jerome, W. G, Fuseler, J, & Price, R. L. Specimen Preparation. In: Price RL., Jerome WG., (ed.) Basic Confocal Microscopy. Springer; (2011). , 61-77.

[20] Tsienv, R. Y, Ernst, L, & Waggoner, A. Fluorophores for Confocal Microscopy: Photophysics and Photochemistry. In: Pawley JB. (ed.) Handbook of Biological Confocal Microscopy. Springer Science Business Media; (2006). , 338-352.

[21] Souza, J. G, Gelfuso, G. M, Simão, P. S, & Borges, A. C. Lopez RFV. Iontophoretic transport of zinc phthalocyanine tetrasulfonic acid as a tool to improve drug topical delivery. Anti-Cancer Drugs (2011).

[22] Manconi, M, Caddeo, C, Sinico, C, Valenti, D, Mostallino, M. C, Biggio, G, & Fadda, A. M. Ex vivo skin delivery of diclofenac by transcutol containing liposomes and suggested mechanism of vesicle-skin interaction. European Journal of Pharmaceutics and Biopharmaceutics (2011).

[23] Manconi, M, Caddeo, C, Sinico, C, Valenti, D, Mostallino, M. C, Lampis, S, Monduzzi, M, & Fadda, A. M. Penetration enhancer-containing vesicles: Composition dependence of structural features and skin penetration ability. European Journal of Pharmaceutics and Biopharmaceutics (2012).

[24] Grams, Y. Y, Alaruikka, S, Lashley, L, Caussin, J, Whitehead, L, & Bouwstr, J. A. Permeant lipophilicity and vehicle composition influence accumulation of dyes in hair follicles of human skin. European Journal of Pharmaceutical Sciences (2003).

[25] Herwadkar, A, Sachdeva, V, Taylor, L. F, Silver, H, & Banga, A. K. Low frequency sonophoresis mediated transdermal and intradermal delivery of ketoprofen. International Journal of Pharmaceutics (2012).

[26] Gillet, A, Lecomte, F, Hubert, P, Ducat, E, Evrard, B, & Piel, G. Skin penetration behaviour of liposomes as a function of their composition. European Journal of Pharmaceutics and Biopharmaceutics (2011).

[27] Zhang, W, Gao, J, Zhu, Q, Zhang, M, Ding, X, Wang, X, Hou, X, Fan, W, Ding, B, Wu, X, Wang, X, & Gao, S. Penetration and distribution of PLGA nanoparticles in the human skin treated with microneedles. International Journal of Pharmaceutics (2010).

[28] Patlolla, R. R, Desai, P. R, Belay, K, & Singh, M. S. Translocation of cell penetrating peptide engrafted nanoparticles across skin layers. Biomaterials (2010).

[29] Shah, P. P, Desai, P. R, & Singh, M. Effect of oleic acid modified polymeric bilayered nanoparticles on percutaneous delivery of spantide II and ketoprofen. Journal of Controlled Release (2012).

[30] Shah, P. P, Desai, P. R, Channer, D, & Singh, M. Enhanced skin permeation using polyarginine modified nanostructured lipid carriers. Journal of Controlled Release (2012).

[31] Bachhav, Y. G, Summer, S, Heinrich, A, Bragagna, T, Böhler, C, & Kalia, Y. N. Effect of controlled laser microporation on drug transport kinetics into and across the skin. Journal of Controlled Release (2010).

[32] Morimoto, Y, Mutoh, M, Ueda, H, Fang, L, Hirayama, K, Atobe, M, & Kobayashi, D. Elucidation of the transport pathway in hairless rat skin enhanced by low-frequency sonophoresis based on the solute-water transport relationship and confocal microscopy. Journal of Controlled Release (2005).

[33] Bal, S. M, Kruithof, A. C, Zwier, R, Dietz, E, Bouwstra, J. A, Lademann, J, & Meinke, M. C. Influence of microneedle shape on the transport of a fluorescent dye into human skin *in vivo*. Journal of Controlled Release (2010).

[34] Bachhav, Y. G, Mondon, K, Kalia, Y. N, Gurny, R, & Möller, M. Novel micelle formulations to increase cutaneous bioavailability of azole antifungals. Journal of Controlled Release (2011).

[35] Borowska, K, Wolowiec, S, Rubaj, A, Glowniak, K, Sieniawska, E, & Radej, S. Effect of polyamidoamine dendrimer G3 and G4 on skin permeation of 8-methoxypsoralene-*In vivo* study. International Journal of Pharmaceutics (2012).

[36] Campbell CSJContreras-Rojas LR., Delgado-Charro MB., Guy RH. Objective assessment of nanoparticle disposition in mammalian skin after topical exposure. Journal of Controlled Release (2012).

[37] Gillet, A, Compère, P, Lecomte, F, Hubert, P, Ducat, E, Evrard, B, & Piel, G. Liposome surface charge influence on skin penetration behavior. International Journal of Pharmaceutics (2011).

[38] Park, J, Lee, J, Kim, Y, & Prausnitz, M. R. The effect of heat on skin permeability. International Journal of Pharmaceutics (2008).

[39] Hathout, R. M, Mansour, S, Geneidi, A. S, & Mortada, N. D. Visualization, dermatopharmacokinetic analysis and monitoring the conformational effects of a microemulsion formulation in the skin stratum corneum. Journal of Colloid and Interface Science (2011).

[40] Abdel-Mottaleb MMAMoulari B., Beduneau A., Pellequer Y., Lamprecht A. Nanoparticles enhance therapeutic outcome in inflamed skin therapy. European Journal of Pharmaceutics and Biopharmaceutics (2012).

[41] Zhang, L. W, Yu, W. W, Colvin, V. L, & Monteiro-riviere, N. A. Biological interactions of quantum dot nanoparticles in skin and in human epidermal keratinocytes. Toxicology and Applied Pharmacology (2008).

[42] He, R, Cui, D, & Gao, F. Preparation of fluorescence ethosomes based on quantum dots and their skin scar penetration properties. Materials Letters (2009).

[43] Gratieri, T, Schaefer, U. F, Jing, L, Gao, M, & Kostka, K. H. Lopez RFV., Schneider M. Penetration of Quantum Dot Particles Through Human Skin. Journal of Biomedical Nanotechnology (2010).

[44] Lopez RFVSeto JE., Blankschtein D., Langer R. Enhancing the transdermal delivery of rigid nanoparticles using the simultaneous application of ultrasound and sodium lauryl sulfate. Biomaterials (2011).

[45] Zhang, Z, Wo, Y, Zhang, Y, Wang, D, He, R, Chen, H, & Cui, D. *In vitro* study of ethosome penetration in human skin and hypertrophic scar tissue. Nanomedicine: Nanotechnology, Biology, and Medicine (2012).

[46] Cevc, G, Schätzlein, A, & Richardsen, H. Ultradeformable lipid vesicles can penetrate the skin and other semi-permeable barriers unfragmented. Evidence from double label CLSM experiments and direct size measurements. Biochimica et Biophysica Acta (2002).

[47] Smith, C. L. Basic Confocal Microscopy. Current Protocols in Neuroscience (2011). , 1-2.

[48] Claxton, N. S, Fellers, T. J, & Davidson, M. W. Microscopy, Confocal. Encyclopedia of Medical Devices and Instrumentation (2006). , 1-37.

[49] Lademann, J, Otberg, N, Richter, H, Meyer, L, Audring, H, Teichmann, A, Thomas, S, Knüttel, A, & Sterry, W. Application of optical non-invasive methods in skin physiology: a comparison of laser scanning microscopy and optical coherent tomography with histological analysis. Skin Research and Technology (2007).

[50] Meyer, L. E, Otberg, N, Sterry, W, & Lademann, J. *In vivo* confocal scanning laser microscopy: comparison of the reflectance and fluorescence mode by imaging human skin. Journal of Biomedical Optics (2006). , 11(4), 0440121-0440127.

[51] González, S, & Gilaberte-calzada, Y. *In vivo* reflectance-mode confocal microscopy in clinical dermatology and cosmetology. International Journal of Cosmetic Science (2008).

[52] Angelova-fischer, I, Pfeuti, T, Zillikens, D, & Rose, C. *In vivo* confocal laser scanning microscopy for non-invasive diagnosis of pemphigus foliaceus. Skin Research and Technology (2009).

[53] Koehler, M. J, Speicher, M, Lange-asschenfeldt, S, Stockfleth, E, Metz, S, Elsner, P, Kaatz, M, & König, K. Clinical application of multiphoton tomography in combination with confocal laser scanning microscopy for *in vivo* evaluation of skin diseases. Experimental Dermatology (2011).

[54] González, S. Confocal Reflectance Microscopy in Dermatology: Promise and Reality of Non-Invasive Diagnosis and Monitoring. Actas Dermosifiliogr (2009).

[55] Fan, C, Luedtke, M. A, Prouty, S. M, Burrows, M, Kollias, N, & Cotsarelis, G. Characterization and quantification of wound-induced hair follicle neogenesis using *in vivo* confocal scanning laser microscopy. Skin Research and Technology (2011).

[56] Ahad, A, Aqil, M, Kohli, K, Sultana, Y, Mujeeb, M, & Ali, A. Formulation and optimization of nanotransfersomes using experimental design technique for accentuated transdermal delivery of valsartan. Nanomedicine: Nanotechnology, Biology, and Medicine (2012).

[57] Rastogi, R, Anand, S, & Koul, V. Flexible polymerosomes-An alternative vehicle for topical delivery. Colloids and Surfaces B: Biointerfaces (2009).

[58] Teixeira, Z, Zanchetta, B, Melo, B. A. G, Oliveira, L. L, Santana, M. H. A, Paredes-gamero, E. J, Justo, G. Z, Nader, H. B, Guterres, S. S, & Durán, N. Retinyl palmitate flexible polymeric nanocapsules: Characterization and permeation studies.Colloids and Surfaces B: Biointerfaces (2010).

[59] Stracke, F, Weiss, B, Lehr, C. M, Konig, K, Schaefer, U. F, & Schneider, M. Multiphoton Microscopy for the Investigation of Dermal Penetration of Nanoparticle-Borne Drugs. Journal of Investigative Dermatology doi:sj.jid.5700374. http://www.nature.com/jid/journal/vaop/ncurrent/abs/5700374a.htmlacessed 01 october (2012).

[60] Akhtar, N, Pathak, K, & Cavamax, W. Composite Ethosomal Gel of Clotrimazole for Improved Topical Delivery: Development and Comparison with Ethosomal Gel. AAPS PharmSciTech (2012). , 13(1), 344-355.

[61] Pople, P. V, & Singh, K. K. Targeting tacrolimus to deeper layers of skin with improved safety for treatment of atopic dermatitis. International Journal of Pharmaceutics (2010).

[62] Alvarez-román, R, Naik, A, Kalia, Y. N, Guy, R. H, & Fessi, H. Skin penetration and distribution of polymeric nanoparticles. Journal of Controlled Release (2004).

[63] De Rosa, F. S, Lopez, R. F. V, Thomazini, J. A, Tedesco, A. C, Lange, N, & Bentley, M. V. L. B. *In vitro* Metabolism of 5-ALA Esters Derivatives in Hairless Mice Skin Homo-

genate and *in vivo* PpIX Accumulation Studies. Pharmaceutical Research (2004). , 21(12), 2247-2252.

[64] Fang, Y, Tsai, Y, Wu, P, & Huang, Y. Comparison of aminolevulinic acid-encapsulated liposome versus ethosome for skin delivery for photodynamic therapy. International Journal of Pharmaceutics (2008). , 5.

[65] Lanke, S. S. S, Kolli, C. S, Strom, J. G, & Banga, A. K. Enhanced transdermal delivery of low molecular weight heparin by barrier perturbation. International Journal of Pharmaceutics (2009).

[66] Lee, W, Shen, S, Al-suwayeh, S. A, Yang, H, Yuan, C, & Fang, J. Laser-assisted topical drug delivery by using a low-fluence fractional laser: Imiquimod and macromolecules. Journal of Controlled Release (2011).

[67] Gerger, A, Wellenhof, R. H, Samonigg, H, & Smolle, J. *In vivo* confocal laser scanning microscopy in the diagnosis of melanocytic skin tumours. British Journal of Dermatology (2009).

[68] Rajadhyaksha, M, Grossman, M, Esterowitz, D, Webb, R. H, & Anderson, R. R. *In vivo* confocal scanning laser microscopy of human skin: melanin provides strong contrast. Journal of Investigative Dermatology (1995).

[69] Nori, S, Rius-díaz, F, Cuevas, J, Goldgeier, M, Jaen, P, Torres, A, & González, S. Sensitivity and specificity of reflectance-mode confocal microscopy for *in vivo* diagnosis of basal cell carcinoma: A multicenter study. Journal of the American Acaddemy of Dermatology (2004).

[70] Guitera, P, Pellacani, G, Crotty, K. A, Scolyer, R. A, Li, L, Bassoli, S, Vinceti, M, Rabinovitz, H, Longo, C, & Menzies, S. W. The Impact of *In vivo* Reflectance Confocal Microscopy on the Diagnostic Accuracy of Lentigo Maligna and Equivocal Pigmented and Nonpigmented Macules of the Face. Journal of Investigative Dermatology (2010).

[71] Koller, S, Gerger, A, Ahlgrimm-siess, V, Weger, W, Smolle, J, & Hofmann-wellenhof, R. *In vivo* reflectance confocal microscopy of erythematosquamous skin diseases. Experimental Dermatology (2009).

[72] Kurzeja, M, Rakowska, A, Rudnicka, L, & Olszewska, M. Criteria for diagnosing pemphigus vulgaris and pemphigus foliaceus by reflectance confocal microscopy. Skin Research and Technology (2012).

[73] Ulrich, M, Krueger-corcoran, D, Roewert-huber, J, Sterry, W, Stockfleth, E, & Astner, S. Reflectance confocal microscopy for noninvasive monitoring of therapy and detection of subclinical actinic keratoses. Dermatology (2010). , 220(1), 15-24.

[74] Langley, R. G. B, Rajadhyaksha, M, Dwyer, P. J, Sober, A. J, Flotte, T. J, & Anderson, R. R. Confocal scanning laser microscopy of benign and malignant melanocytic skin lesions *in vivo*. Journal of the American Academy of Dermatology (2001).

[75] Langley, R. G. B, Burton, E, Walsh, N, Propperova, I, & Murray, S. J. *In vivo* confocal scanning laser microscopy of benign lentigines: comparison to conventional histology and *in vivo* characteristics of lentigo maligna. Journal of the American Academy of Dermatology (2006).

[76] Swindells, K, Burnett, N, Rius-diaz, F, González, E, Mihm, M. C, & González, S. Reflectance confocal microscopy may differentiate acute allergic and irritant contact dermatitis *in vivo*. Journal of the American Academy of Dermatology (2004).

[77] González, S, González, E, White, M, Rajadhyaksha, M, & Anderson, R. R. Allergic contact dermatitis: Correlation of *in vivo* confocal imaging to routine histology. Journal of the American Academy of Dermatology (1999a).

[78] Aghassi, D, Anderson, R. R, & González, S. Confocal laser microscopic imaging of actinic keratoses *in vivo*: A preliminary report.Journal of the American Academy of Dermatology (2000).

[79] Astner, S, González, E, Cheung, A, Díaz, F. R, Doukas, A. G, William, F, & González, S. Non-invasive evaluation of the kinetics of allergic and irritant contact dermatitis. Journal of Investigative Dermatology (2005).

[80] Ferris, L. K, & Harris, R. J. New Diagnostic Aids for Melanoma. Dermatologic Clinics (2012).

[81] Gerger, A, Koller, S, Kern, T, Massone, C, Steiger, K, Richtig, E, Kerl, H, & Smolle, J. Diagnostic applicability of *in vivo* confocal laser scanning microscopy in melanocytic skin tumors. Journal of Investigative Dermatology (2005).

[82] Pellacani, G, Cesinaro, A. M, & Seidenari, S. Reflectance-mode confocal microscopy of pigmented skin lesions-improvement in melanoma diagnostic specificity. Journal of the American Academy of Dermatology (2005a).

[83] Pellacani, G, Cesinaro, A. M, & Seidenari, S. *In vivo* assessment of melanocytic nests in nevi and melanomas by reflectance confocal microscopy. Modern Pathology (2005b).

[84] Pellacani, G, Guitera, P, Longo, C, Avramidis, M, Seidenari, S, & Menzies, S. The impact of *in vivo* reflectance confocal microscopy for the diagnostic accuracy of melanoma and equivocal melanocytic lesions. Journal of Investigative Dermatology (2007).

[85] Ahlgrimm-siess, V, Massone, C, Scope, A, Fink-punches, A, Richtig, E, Wolf, I. H, Koller, S, Gerger, A, Smolle, J, & Hoffmann-wellenhor, R. Reflectance confocal microscopy of facial lentigo maligna and lentigo maligna melanoma: a preliminary study. British Journal of Dermatology (2009).

[86] Busam, K. J, Hester, K, Charles, C, Sachs, D. L, Antonescu, C. R, Gonzalez, S, & Halpern, A. C. Detection of clinically amelanotic malignant melanoma and assessment of its margins by *in vivo* confocal scanning laser microscopy. Archives of Dermatology (2001).

[87] Curiel-lewandrowski, C, Williams, C. M, Swindells, K. J, Tahan, S. R, Astner, S, Frankenthaler, R. A, & González, S. Use of *in vivo* confocal microscopy in malignant melanoma: an aid in diagnosis and assessment of surgical and nonsurgical therapeutic approaches. Archives of Dermatology (2004).

[88] Ulrich, M, Maltusch, A, Röwert-huber, J, González, S, Sterry, W, Stockfleth, E, & Astner, S. Actinic keratoses: non-invasive diagnosis for field cancerisation. British Journal of Dermatology (2007). , 156(3), 13-7.

[89] Ulrich, M, Maltusch, A, Rius-diaz, F, Röwert-huber, J, González, S, Sterry, W, Stockfleth, E, & Astner, S. Clinical applicability of *in vivo* reflectance confocal microscopy for the diagnosis of actinic keratoses. Dermatologic Surgery (2008).

[90] Rishpon, A, Kim, N, Scope, A, Porges, L, Oliviero, M. C, Braun, R. P, Marghoob, A. A, Fox, C. A, & Rabinovitz, H. S. Reflectance Confocal Microscopy Criteria for Squamous Cell Carcinomas and Actinic Keratoses. Archives of Dermatology (2009). , 145(7), 766-772.

[91] González, S, & Tannous, Z. Real-time, *in vivo* confocal reflectance microscopy of basal cell carcinoma. Journal of American Academy of Dermatology (2002).

[92] Sauermann, K, Gambichler, T, Wilmert, M, Rotterdam, S, Stücker, M, Altmeyer, P, & Hoffmann, K. Investigation of basal cell carcinoma by confocal laser scanning microscopy *in vivo*. Skin Research and Technolgy (2002).

[93] Astner, S, Dietterle, S, Otberg, N, Röwert-huber, H. J, Stockfleth, E, & Lademann, J. Clinical applicability of *in vivo* fluorescence confocal microscopy for noninvasive diagnosis and therapeutic monitoring of nonmelanoma skin cancer. Journal of Biomedical Optics (2008).

[94] Ulrich, M, Lange-asschenfeldt, S, & González, S. *In vivo* reflectance confocal microscopy for early diagnosis of nonmelanoma skin cancer. Actas Dermosifiliográficas (2012). http://dx.doi.org/10.1016/j.ad.2011.10.017.

[95] Wu, X, Xu, A, Song, X, Zheng, J, Wang, P, & Shen, H. Clinical, pathologic, and ultrastructural studies of progressive macular hypomelanosis. International Journal of Dermatology (2010).

[96] Chiaverini, C, Kang, H, Sillard, L, Berard, E, Niaudet, P, Guest, G, Cailliez, M, Bahadoran, P, Lacour, J. P, Ballotti, R, & Ortonne, J. P. *In vivo* reflectance confocal microscopy of the skin: A noninvasive means of assessing body cystine accumulation in infantile cystinosis. Journal of the American Academy of Dermatology 10.1016/j.jaad. (2011).

[97] González, S, Rajadhyasksha, M, Rubinstein, G, & Anderson, R. R. Characterization of psoriasis *in vivo* by confocal reflectance microscopy. Journal of Medicine (1999).

[98] Ardigo, M, Cota, C, Berardesca, E, & González, S. Concordance between *in vivo* reflectance confocal microscopy and histology in the evaluation of plaque psoriasis. Journal of the European Academy of Dermatology and Venereology (2009).

[99] Wolberink, E. A. W, Van Erp, P. E. J, & Teussink, M. M. van de Kerkhof P.C.M., Gerritsen M.J.P. Cellular featuresof psoriatic skin: imaging and quantification using *in vivo* reflectance confocal microscopy. Cytometry Part B (2011). B) , 141-149.

[100] González, S, White, W. M, Rajadhyaksha, M, Anderson, R. R, & González, E. Confocal Imaging of Sebaceous Gland Hyperplasia *In vivo* to Assess Efficacy and Mechanism of Pulsed Dye Laser Treatment. Lasers in Surgery and Medicine (1999b).

[101] Aghassi, D, González, E, Anderson, R. R, Rajadhyaksha, M, & González, S. Elucidating the pulsed-dye laser treatment of sebaceous hyperplasia *in vivo* with real-time confocal scanning laser microscopy. Journal of the American Academy of Dermatology (2000b).

[102] Propperova, I, & Langley, R. G. B. Reflectance-Mode Confocal Microscopy for the Diagnosis of Sebaceous Hyperplasia *In vivo*. Archives of Dermatology (2007).

[103] Agero, A. L, Gill, M, Ardigo, M, Myskowski, P, Halpern, A. C, & González, S. *In vivo* reflectance confocal microscopy of mycosis fungoides: a preliminary study. Journal of the American Academy of Dermatology (2007).

[104] Lange-asschenfeldt, S, Babilli, J, Beyer, M, Ríus-diaz, F, González, S, Stockfleth, E, & Ulrich, M. Consistency and distribution of reflectance confocal microscopy features for diagnosis of cutaneous T cell lymphoma. Journal of Biomedical Optics (2012).

[105] Ardigo, M, Zieff, J, Scope, A, Gill, M, Spencer, P, Deng, L, & Marghoob, A. A. Dermoscopic and reflectance confocal microscope findings of trichoepithelioma. Dermatology (2007).

[106] Hongcharu, W, Dwyer, P, González, S, & Anderson, R. R. Confirmation of onychomychosis by confocal microscopy. Journal of the American Academy of Dermatology (2000).

[107] Turan, E, Erdemir, A. T, Gurel, M. S, & Yurt, N. A new diagnostic technique for tinea incognito: *In vivo* reflectance confocal microscopy. Report of five cases. Skin Research and Technology (2012). Jun 7. doi:j.x., 1600-0846.

[108] Hui, D, Xue-cheng, S, & Ai-e, X. Evaluation of reflectance confocal microscopy in dermatophytosis. Mycoses (2012). Sep 10. doi:j.x, 1439-0507.

[109] Kreuter, A, Gambichler, T, Sauermann, K, Jansen, T, Altmeyer, P, & Hoffmann, K. Extragenital lichen sclerosus successfully treated with topical calcipotriol: evaluation by *in vivo* confocal scanning laser microscopy. British Journal of Dermatology (2002).

[110] González, S, Rajadhyaksha, M, González-serva, A, White, W. M, & Anderson, R. R. Confocal reflectance imaging of folliculitis *in vivo*: correlation with routine histology. Journal of Cutaneous Pathology (1999c).

[111] Scheuplein, R. J, & Blank, I. H. Permeability of the skin. Physiological Reviews (1971).

[112] Elias, P. M. Epidermal lipids, barrier function, and desquamation. Journal of Investigative Dermatology (1983). s-49s.

[113] Desai, P, Patlolla, R. R, & Singh, M. Interaction of nanoparticles and cell-penetrating peptides with skin for transdermal drug delivery. Molecular Membrane Biology (2010). , 27(7), 247-259.

[114] Foldvari, M, Badea, I, Wettig, S, Baboolal, D, Kumar, P, Creagh, A. L, & Haynes, C. A. Topical Delivery of Interferon Alpha by Biphasic Vesicles: Evidence for a Novel Nanopathway across the Stratum Corneum. Molecular Pharmaceutics (2010). , 7(3), 751-762.

[115] Teeranachaideekul, V, Boonme, P, Souto, E. B, Müller, R. H, & Junyaprasert, V. B. Influence of oil content on physicochemical properties and skin distribution of Nile red-loaded NLC. Journal of Controlled Release (2008). , 128(2), 134-41.

[116] Madsen, H. B, Ifversen, P, Madsen, F, Brodin, B, Hausser, I, & Nielsen, H. M. *In vitro* Cutaneous Application of ISCOMs on Human Skin Enhances Delivery of Hydrophobic Model Compounds Through the Stratum Corneum. The AAPS Journal (2009). , 11(4), 728-739.

[117] Lopez-pinto, J. M, Gonzalez-rodriguez, M. L, & Rabasco, A. M. Effect of cholesterol and ethanol on dermal delivery from DPPC liposomes. International Journal of Pharmaceutics (2005).

[118] Lademann, J, Richter, H, Teichmann, A, Otberg, N, Blume-peytavi, U, Luengo, J, Wei, B, Schaefer, U. F, Lehr, C. M, Wepf, R, & Sterry, W. Nanoparticles- An efficient carrier for drug delivery into the hair follicles. European Journal of Pharmaceutics and Biopharmaceutics (2007).

[119] Van Kuijk-meuwissen, M, Mougin, L, Junginger, H. E, & Bouwstra, J. A. Application of vesicles to rat skin *in vivo*: a confocal laser scanning microscopy study. Journal of Controlled Release (1998).

[120] Godin, B, & Touitou, E. Mechanism of bacitracin permeation enhancement through the skin and cellular membranes from an ethosomal carrier. Journal of Controlled Release (2004).

[121] Regnier, V, & Préat, V. Localization of a FITC-labeled phosphorothioate oligodeoxynucleotide in the skin after topical delivery by iontophoresis and electroporation. Pharmaceutical Research (1998). , 15(10), 1596-602.

[122] Prausnitz, M. R, Gimm, J. A, Guy, R. H, Langer, R, Weaver, J. C, & Cullander, C. Imaging Regions of Transport across Human Stratum Corneum during High-Voltage

and Low-Voltage Exposures. Journal of Pharmaceutical Sciences (1996). , 85(12), 1363-1370.

[123] Seto, J. E, Polat, B. E, Lopez, R. F. V, Blankschtein, D, & Langer, R. Effects of ultrasound and sodium lauryl sulfate on the transdermal delivery of hydrophilic permeants: Comparative *in vitro* studies with full-thickness and split-thickness pig and human skin. Journal of Controlled Release (2010). , 145(1), 26-32.

[124] Dubey, V, Mishra, D, Asthana, A, & Jain, N. K. Transdermal delivery of a pineal hormone: Melatonin via elastic liposomes. Biomaterials (2006).